MODELLING AND MEASUREMENT OF RADON DIFFUSION THROUGH SOIL FOR APPLICATION ON MINE TAILINGS DAMS

WILCOT JOHN SPEELMAN

A thesis submitted in partial fulfillment of the requirements for the degree of Magister Scientiae in the Faculty of Natural Sciences, University of the Western Cape.

Supervisor : Prof R. Lindsay

December 2004

MODELLING AND MEASUREMENT OF RADON DIFFUSION THROUGH SOIL FOR APPLICATION ON MINE TAILINGS DAMS

Wilcot John Speelman

Keywords

^{222}Rn

^{226}Ra

Electret

Diffusion

Emanation

RAD7™

E-PERM®

Radiation

Modelling

Tailings dam

Declaration:

I, the undersigned, declare that the work contained in this thesis, **Modelling and Measurement of Radon Diffusion Through Soil For Application On Mine Tailings Dams**, is my original work and has not previously in its entirety or part been submitted at any university for a degree, and that all the sources I have used or quoted have been indicated and acknowledged by complete references.

Wilcot John Speelman December 2004

Signature: .....

ACKNOWLEDGEMENTS

I would like to take this oppurtunity to acknowledge the following people and institutions for their invaluable support while conducting the study as well as through the writing process:

Prof Robbie Lindsay, supervisor, for his guidance, mental and technical support as well as financial contribution and willingness to always help in the completion of this study,

the **staff and students at the Environmental Radioactivity Laboratory at iThemba LABS**, especially Dr Richard Newman, Angelo Joseph, Pogisho Maine, Wesley Damon and Katse Maphoto, for the provision of technical equipment and assistance throughout the study,

Prof Rob de Meijer, for his valuable input on the experimental setup and data analysis,

the **Physics Department of UWC**, for the kind support and assistance throughout the course of the study,

the financial contribution from the **National Research Foundation** through the **Department of Labour Scarce Skills Master's Scholarship**,

my **parents, Ivor and aunty Betty**, and my **family** and **friends** for their support, love and encouragement throughout,

and lastly, but not the least, **Hazel**, for her undying love and support, who was with me, right from the beginning, thank you very much.

ABSTRACT

MODELLING AND MEASUREMENT OF RADON DIFFUSION THROUGH SOIL FOR APPLICATION ON MINE TAILINGS DAMS

Wilcot J. Speelman

M.Sc full thesis, Department of Physics, University of the Western Cape

Radon (^{222}Rn) has been identified as an important factor that could result in a health hazard by studies all around the world. The health risks can be minimised by preventive measures where radon is highly concentrated as in some mines and homes. A study in the diffusion of the inert gas, will give us a better understanding of its possible pathways through soil into the air surrounding mine dumps where the radon releases can become hazardous. Measuring and modelling the radon concentrations in the mine dump soil, can help to deduce the radon flux to identify the problem areas for rehabilitation especially in the cases of gold and uranium mine tailings. Rehabilitation in those cases usually consists of a multilayer cover of solids like crushed rock or clay. A passive method incorporating electret technology is used in this study to determine the radon emanation coefficient of the soil. Emanation coefficients ranging from 0.13 to 0.39 have been obtained. The scope of this investigation also describes the modelling of a depth profile with respect to the radon activity concentration to understand from how deep radon might be migrating, as well as the effect of different diffusion lengths. An actual depth profile is presented, measured with a continuous radon monitor, the RAD7™. Several hundreds of kBq/m^3 of radon soil gas concentration are recorded at depths of about 1.2 meters.

Contents

Chapter 1

Motivation for the study

1.1 Introduction

Mine tailings dams have been around since the discovery of precious metals. These massive amounts of earthen materials need to be dumped somewhere and a good strategy need to be advised to engineer a place to dump these wastes. These tailings are the result of processing for rare or precious metals. The ore is processed with chemicals like arsenic or cyanide for separation of the metals from the ore. The unused parts are then dumped in huge dams constructed to store the tailings from these processing plants. The tailings dams are usually located in fairly inaccessible areas to the public but sometimes are very close to residential areas that resulted from population growth factors and land issues. This study will discuss some aspects of the mine tailings dams, which forms part of a study of the possible radiological impact of the dams.

The dump sites are engineered in such a way that they should have as little impact on the environment as possible and the remediation of such tailings dams is very important. Rehabilitation of the dump sites in some countries involves a series of compact layers of solids on top of the processed ore [Bra03]. Examples of the development to minimise the risk of contamination to the environment as well as humans are the application of a variety of solids that include soils of different porosities, densities and texture. These layers are integral to the integrity of the mine dump and could prevent disasters of a

large extent through slimes spillage or possible radiation exposure from ionising radiation originating from the dump itself.

Examples of the function of the earthen cover materials are listed below:

- Surface layer
- Drainage layer
- Waterproofing layer (barrier)
- Gas collecting layer

Not all the above mentioned layers will be applied as a barrier of protection, but some combination thereof. No earthen layers like the above mentioned ones are being applied to mine dumps in South Africa, and herein lays the problem from a radiological sense. These will be discussed later in this study. The soil used in the rehabilitation is important to perform a number of tasks on the site. The quality of the soil with respect to radioactivity concentrations of the following natural occurring radionuclides; ^{238}U, ^{40}K and ^{232}Th are of prime importance when characterising the soil from a radiological point of view. Since these nuclides are radioactive and because they have different half-lives, they decay to progenies that are of great importance for studies of mine dumps. The most notable one is the production of ^{222}Rn (Radon, hereafter just Rn) in the ^{238}U Decay Series. Radon brings about its own set of progenies that are potentially hazardous [Jam88] to humans and because of this potential danger and the fact that it is an inert gas, a study is necessary into the transport and diffusion properties of Rn on a mine dump.

1.2 Background

Henri Becquerel discovered radioactivity in 1896 [Seg80] by experimenting with uranium. He discovered that the uranium continuously emitted “radiation”

and he also wanted to know whether this feature was only common to uranium or other elements as well. Pierre and Marie Curie then joined the study of radioactivity (proposed by Marie Curie) in 1897 and they found that the elements radium, thorium and polonium shared the same effect that Henri Becquerel was investigating. Right about the same time, Ernest Rutherford was also conducting research on radioactivity and in the year 1898, he confirmed Becquerel's findings. The continuous emission of radiation, he identified as two different types; the relatively easy absorbed 'alpha' rays and the more penetrating 'beta' rays. He also went on to show that these rays had a particle nature [Cam02].

In 1900, Friedrich Ernst Dorn discovered that radium emanates a gas that was first called 'Niton' (the Latin word for nitens which means shining). This gas was later to be named radon in 1923. William Ramsay and Robert Whytlaw-Gray isolated radon in 1908 [Wik04] and determined its density. They found that it was the heaviest known gas. In 1902, Marie and Pierre Curie isolated the radioactive element radium. Henri Becquerel, together with Pierre and Marie Curie shared the Physics Nobel Prize in 1903 for their work on radioactivity. Marie Curie was also awarded the Chemistry Nobel Prize in 1911 for the discovery of the elements polonium and radium.

1.3 Overview of Radon

Radon (^{222}Rn) is the radioactive gas with atomic number 86 and atomic weight of 222. It has no colour, it is odourless and it is the heaviest noble gas at room temperature. It is the result of the radioactive decay ^{226}Ra by

emission of an alpha particle in the ^{238}U decay series. It has a half-life of 3.82 days.

There exist quite a few other isotopes of radon besides ^{222}Rn; the most notable ones are ^{220}Rn that is known as thoron and ^{219}Rn, which is known as actinon. Thoron is formed in the thorium (^{232}Th) decay series wherein ^{224}Ra decays to form it. Thoron has a half-life 55.6 seconds. Actinon on the other hand is formed in the ^{235}U decay series when ^{223}Ra decays to actinon. Actinon has a half-life of about 3.96 seconds. Radon-222's lifetime is considered long relative to the other isotopes. This is of significance, since radon is formed in the ground or building materials [Ner88] and has significantly more time to diffuse through the material into the indoor environment in buildings or the outdoor atmosphere.

The radon formed relatively close to the earth's surface can diffuse through the soil or be driven by pressure gradients [Sam84]. The question that is raised is from what depth the radon atoms are coming. Considering the outdoor release of radon, say for instance on a mine dump, it is of less radiological significance than the indoor problem, but the diffusion mechanisms and transport routes of the gas in the soil is of more importance.

1.4 Motivation for Study of Radon on Mine Dumps

Radon is the decay result of ^{226}Ra and radon in turn decays by alpha emission to ^{218}Po, which further decays to ^{214}Pb, and the process continues down a long decay chain (Fig.2.1). The elements following radon are called progeny of radon known as radon daughters. They are chemically active and they have relatively short half-lives [Ner88]. If humans are exposed to the

radon, the gas itself can be inhaled or exhaled, and if the decay probability of radon is high enough, the progeny resulting from the decay chain might stick to the lungs. They also might end up via a different mechanism in the lung cavities or on the lungs; the inhalation of the progeny that stick to dust or aerosol particles in the air has been identified as by far the most important pathway [God02]. Radiation gets released when these progenies decay on the surface of the lung and imparts the lung dose that increases the risk of inducing lung cancer [Wil00].

Mine tailings sites carry the potential to induce a similar risk to cause lung cancer as a result of the large quantity of radon released from the slimes dams. It follows from the historical evidence that radon decay products are associated with health risks to the underground mining population of Scheeberg (Germany) and St Joachimstahl (Bohemia) in the sixteenth century [Ste88]. That is the precedent for the health implications for underground mining. The mine tailings from ore processing is different in the sense that there is no build up on the dump itself like the problems of very high activity concentrations [Ste88] of radon that the early underground miners were exposed to. Homes or dwellings situated close to these mine dumps, may result in radon build up. To understand the processes by which the radon migrates to the soil-air interface where it is available to disperse readily, in-situ activity concentration measurements were done on the tailings dam, investigating the dump site as radon source material. Radiometric analysis on soil samples collected on the dump site will help to determine the emanation factor of radon which is the fraction of the total amount of radon that is produced, that escapes the soil particle where it is formed. Theoretical calculations and modelling of the radon activity concentrations will give insight into the question from how deep radon is migrating (diffusion length) and to

compare with the experimental data.

1.5 The Problem of Radiation from Mine Dumps

Huge mine tailings dams are constructed every year to host the waste from mineral processing around the gold mines in South Africa. These dams can cover areas of some square kilometers of land. The residual material contains radioactive atoms that are found in the rock itself since the gold bearing ore is often associated with high uranium activity. So, these tailings can be seen as a very large source of relatively weak radioactivity [Lin04], which needs to be regulated. The physical and chemical composition of the wastes varies widely; e.g. activity concentrations and the half-lives of the different radionuclides that are present in the processed ores. The type of radioactive wastes generated from mining and milling of the ores include ^{238}U, ^{40}K and ^{232}Th and their decay products. Radon is the most notable decay product from a radiological point of view.

Most mine dump sites are situated on mining property or close to the processing plant, which makes the mining company responsible if anything should happen on the mine dump or nearby that threatens the integrity of the dump itself. Legislation in South Africa addresses the issue of responsible waste management through the 'Radioactive Waste Management Policy and Strategy for the Republic of South Africa' instigated by the Department of Minerals and Energy [Nuclear Energy Act, 1999 (Act No. 46 of 1999)].

The national authority responsible for exercising regulatory control over the radioactivity resulting from mining and minerals processing is the National Nuclear Regulator (NNR). It is almost impossible to fully regulate all these

tailings that might lead to harmful effects arising from the exposure of ionising radiation. Mining sites can become ownerless and through miscommunication the sites might be used for housing purposes or even agriculture. Stark possibilities, but not an impossible eventuality. Future generations would then have to bear the burden. Therefore, characteristic studies of mine dumps ought to be done now, not only to assess the risk for regulation and safety purposes, but also for future references and regulatory control in such a way that the exposure levels are within acceptable levels.

Gamma-ray studies have been done on mine tailings [Lin04] up to now, in assessing gold mine dumps in South Africa, as well as study the feasibility of the method proposed by Lindsay et al. in measuring the radon exhalation from a mine dump. This is done by means of gamma-ray mapping with an in-situ γ-ray detector called MEDUSA (Multi-element Detector system for Underwater Sediment Activity). It uses a CsI(Na) crystal setup that is mounted on to a 4×4 vehicle, together with a GPS device, to record a γ-ray spectrum at various positions, and that would form the basis of the map.

The determination of the radon flux includes parameters like the radon emanation coefficient, the bulk or specific densities of the soil, the porosity as well as the radium activity concentration. The present thesis forms part of this study of the radiological impact of the mine dumps conducted by University of the Western Cape (UWC) and iThemba LABS. It will focus on the determination of the radon emanation coefficient, the specific and bulk densities, the total porosity and briefly discuss the approximate determination of the radium content of the mine soil. Most of these procedures will be conducted in the laboratory at UWC and iThemba LABS. However, an in situ

method of measuring the radon soil-gas will also be used in this study to determine the radon soil-gas potential, and it might also shed some light on the diffusion length inside these mine dumps (depending on the different parameters noted above). This will be coordinated in such a way to also assess the radon concentration at different depths. These results will then be correlated to that of a numerical model that will be formulated. However, certain assumptions will have to be made regarding the parameters used in the modelling for a radon depth profile. The results will then be presented and discussed, followed by the conclusion.

Chapter 2

Mine Tailings and Soil as a Source of Radon and the Production of Radon in Soil

2.1 Introduction

Soil and rock have been identified to be sources of radon [Mar92][Åke97] as well as building materials [Nie96][Bos03]. Mine dumps, as explained in Chapter 1 are tonnes of processed waste product from the mineral processing plants. Once the rock containing the ore is crushed and treated with chemicals like cyanide to extract the minerals; in this case gold, the residue is dumped in huge constructed dams to hold and dry out the waste. These wastes may leave the natural occurring radioactive element uranium and other trace elements enhanced in activity concentrations [Dem01].

The waste will also contain some of the other natural radioactive elements such as thorium (^{232}Th), potassium (^{40}K), uranium (^{238}U) and one of the uranium isotopes (^{235}U). These elements are radioactive and will decay to form their respective decay products and those will also be present in the soil. In the decay of ^{238}U, several decay products are formed, but the rather interesting one is ^{222}Rn which is a gas that may emanate from the host grain particle that the precursor of radon; ^{226}Ra, is contained in. There are three primary modes of decay whereby radioactive nuclei may transform to form other nuclei. These processes are α, β and γ decays. Unstable nuclei emit α and β particles to obtain a more stable arrangement. Gamma (γ) decay

involves a nucleus in an excited state that decays to the ground state but does not change the nuclear species [Kra88], whereas α and β decay alter the mass number of the nucleus. The energy released from a γ-ray decay is usually in the form of a photon. The energies of the γ-rays range from thousands of electron volts (keV) to a few million electron volts (MeV). Different radioactive nuclei emit characteristic gamma radiation, and so these energies can be identified through γ-ray spectroscopy.

Radon might escape the soil particle by recoil and then by the processes of diffusion and advection, could be transported to the surface of the mine dump. The properties that would influence these processes will be discussed in the following sections as well as the processes whereby radioactive nuclei transform to form other species.

2.2 Radioactive Decay Processes

2.2.1 The Radioactive Decay Law

Radioactive nuclides decay statistically by processes like alpha, beta or gamma decay. A radioactive element will not release all particles at once. The decay process is statistical in nature, early researchers came to the realisation that it was impossible to predict when a specific atom would disintegrate to form another. This led to the following deductions. If there exist a number, N of radioactive nuclei at a certain time t, and no new nuclei are being formed in that sample, then the decay (*dN*) in the sample in a certain time (*dt),* would be proportional to the total number of nuclei N in the following way

$$\frac{dN}{dt} = -\lambda N \qquad (2.1)$$

where λ (s^{-1}) is called the decay constant of a specific radioactive species. Equation (2.1) can be rewritten as

$$\lambda = -\frac{(dN/dt)}{N} \qquad (2.2)$$

The above equation explains the nature of λ, which is the probability per unit time for the decay of an atom. The value of λ differs for each nuclide. The solution of equation (2.2) is called the *exponential law of radioactive decay*. It is

$$N(t) = N_0 e^{-\lambda t} \qquad (2.3)$$

where N_0 is the original number of nuclei present at time t = 0.

The above number of nuclei will slowly decay in some cases and faster in other species, but there will be a *statistical* time ($\tau_{1/2}$) after which half of the number of nuclei would have decayed. To get $\tau_{1/2}$, $N = N_0 / 2$ is substituted in equation (2.3) to give

$$\tau_{1/2} = \frac{\ln 2}{\lambda} \qquad (2.4)$$

which is also called the half-life of a species. Typical examples of half-lives are that of radon and radium which are 3.82 days and 1600 years respectively as indicated in Figure 2.1 in the lower part of the boxes.

The activity of a species is expressed in the SI unit Bq (Becquerel, so named after Henri Becquerel) that is defined as 1 disintegration per second. The historical unit that was used is the curie, abbreviated Ci, which is 3.70×10^{10} decays per second and 1Ci was originally the activity of 1 gram of radium.

2.2.2 Alpha Decay

Decay by alpha emission occurs naturally in heavy nuclei in the radioactive series. In the early 20th century, Rutherford's work on α particle scattering led to the realisation that the atom consisted of largely empty space while the nucleus is a relatively large mass in the centre of the atom. He also concluded from his experiments with alpha particles entering a thin-walled chamber, that α particles were in fact helium nuclei [Kra88]. The α emission takes place, because the nucleus gains binding energy from a decrease in the mass of the system. Since the alpha particle is very stable and a relatively tightly bound structure and its mass is relatively small compared to the remaining parts of the nucleus, it is favoured to be emitted from the system together with the release of kinetic energy.

The emission of α particles in these cases is spontaneous and can be stated in the following way

$$ {}^{A}_{Z}X_{N} \rightarrow {}^{A-4}_{Z-2}Y_{N-2} + \alpha \qquad (2.5) $$

where A is the mass number of the nuclear species, Z is the atomic number of the species and N is the number of neutrons. N is not usually indicated in the equation, but could readily be obtained by A-Z. X is the initial decaying nucleus, whereas Y is the final state, and an alpha particle is emitted.
Alpha emission is evident in the ^{238}U nucleus and as an example can be written as

$$ {}^{238}_{92}U \rightarrow {}^{234}_{90}Th + \alpha \qquad (2.6) $$

The final species in equation (2.6) is thorium-234 accompanied with the release of kinetic energy. In Figure 2.1, these energies are indicated in parenthesis in the sketch for that specific alpha decay.

2.2.3 Beta decay

Beta decay occurs when a nucleus decays and gives off a beta particle; which can be an electron or a positron. In the case of electron emission, it is referred to as beta minus decay (β^-) and in the case of a positron, beta plus decay (β^+). Those are the two most basic processes of β decay.

In the beta plus decay process, a proton is converted to a neutron via the weak nuclear force and what comes out is a beta plus particle and a neutrino (see equation 2.8). In β minus decay however, a neutron is converted to a proton via the same weak nuclear force, and the result is a beta minus (β^-) particle as well as an antineutrino (see equation 2.9). Beta decay in the nucleus changes the Z as well as N. This can be represented with the following equation

$$ {}^{A}_{Z}X_{N} \rightarrow {}^{A}_{Z\pm1}Y_{N\pm1} + \beta \qquad (2.7) $$

The process of beta decay leaves the mass number unchanged. Here follows the basic processes [Kra88]

$$ p \rightarrow n + e^+ + \nu \qquad (\beta^+) \qquad (2.8) $$

$$ n \rightarrow p + e^- + \bar{\nu} \qquad (\beta^-) \qquad (2.9) $$

$$ p + e^- \rightarrow n \qquad (\varepsilon) \qquad (2.10) $$

Equation 2.10 depicts the scenario where an orbital electron is captured. The additional particles in equations 2.8 and 2.9 are called the neutrino and the antineutrino respectively. A beta decay is depicted in Figure 2.1 when ^{214}Pb decays to ^{214}Bi.

2.2.4 ^{238}U Decay Series

Radon is formed in the ^{238}U decay series and this chain of events is depicted in Figure 2.1. It undergoes a series of 14 decays to ultimately form a stable nucleus, that of ^{206}Pb. The radon formed in the series is the only radioactive gas in the series and has the longest half-life (3.825 days) relative to its decay products up to the long-lived ^{210}Pb. Since the radon in this instance is contained in a porous material like soil, the time is long enough for the radon gas that is closer to the surface of the soil to be transported there and exhaled to the surrounding atmosphere [Ner88]. The distance it is transported to reach the surface is widely debated and ranges from 1m for some soils [Ner88] to about 1.6-1.9 meters [Søg87].

One other point to notice in the ^{238}U series, is the radionuclides that radon decays to. These have relatively short half-lives and are chemically active. They can attach to airborne particles [God02] like dust and indoor surfaces and respitory tracts [Jam88]. From Fig 2.1, it is evident that most of the decay products, decay via alpha emission and in some cases by beta emission. The energies noted in the figure are in MeV, and the most significant contributors to the lung dose via alpha emission, are radionuclides like ^{218}Po and ^{214}Po with alpha energies of 6.00 and 7.69 Mev respectively.

Table 2.1 Ranges in tissue of α-particles from radon and its decay products [Jam88].

Nuclide	Energy (MeV)	Range (μm)
^{222}Rn	5.49	41
^{218}Po	6.00	48
^{214}Po	7.69	71
^{220}Rn	6.29	52

The vertical arrows pointing downwards represent alpha decay whereas the diagonal arrows upwards indicate beta decays. The decay products of ^{222}Rn in air also have an activity concentration contribution. This is correlated to the potential alpha-energy concentration (PAEC), which gives the overall activity concentrations of the decay products. The PAEC in turn depends on the concentrations of the 3 decay products following radon [Ner88]. The PAEC was introduced in the 1950's in the unit; working level (WL) to implicate safety standards whereby radon decay-product concentrations could be measured in uranium mines. The working level could be expressed in terms of the potential alpha energy as a combination of the radon decay products that amount to 1WL $=2.08\times10^{-5}$Jm^{-3}. One working level corresponds to radon in equilibrium with its decay products with a radon activity concentration of 3700 Bq/m^3 [Ald94]. The decay products carry with them the PAEC and can attach themselves to airborne particles.

The potential risk of developing lung cancer from the decay products listed in Table 2.1 is enhanced through the deposition of it on the sensitive cells in the lungs. The table is listed to show the thickness of the epitheliums in the lung, that plays a role in the understanding of the absorbed dose by those cells [Jam88].

2.2.5 ^{232}Th Decay Series

The ^{232}Th decay series is listed in Fig. 2.2. ^{220}Rn is of prime radiological importance [Ner88], followed by ^{212}Pb and ^{212}Bi with their contribution to the airborne concentrations. In the event of retention in the lung, the ^{212}Bi and ^{212}Po (Fig. 2.2) has a serious irradiation contribution through alpha decay (6.05 and 8.78 MeV respectively) and hence, the health implications. The series is only listed for referencing purposes.

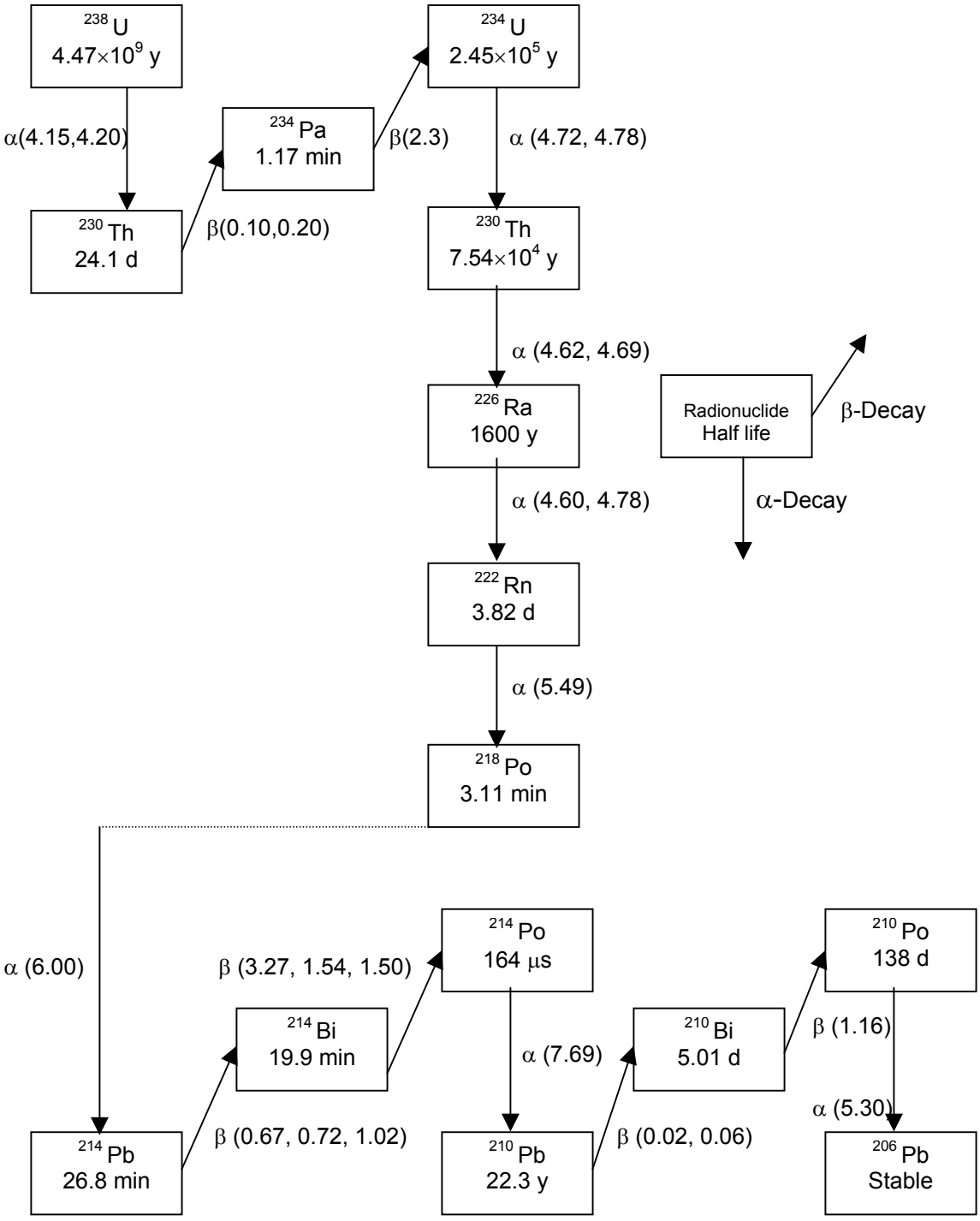

Figure 2.1. Schematic representation of the ^{238}U decay series, including ^{222}Rn as well as its decay products. As the legend suggests, arrows pointing downwards, indicate alpha decay whereas the diagonal arrows indicate beta decay. Alpha and beta energies are given in brackets in MeV [Ner88].

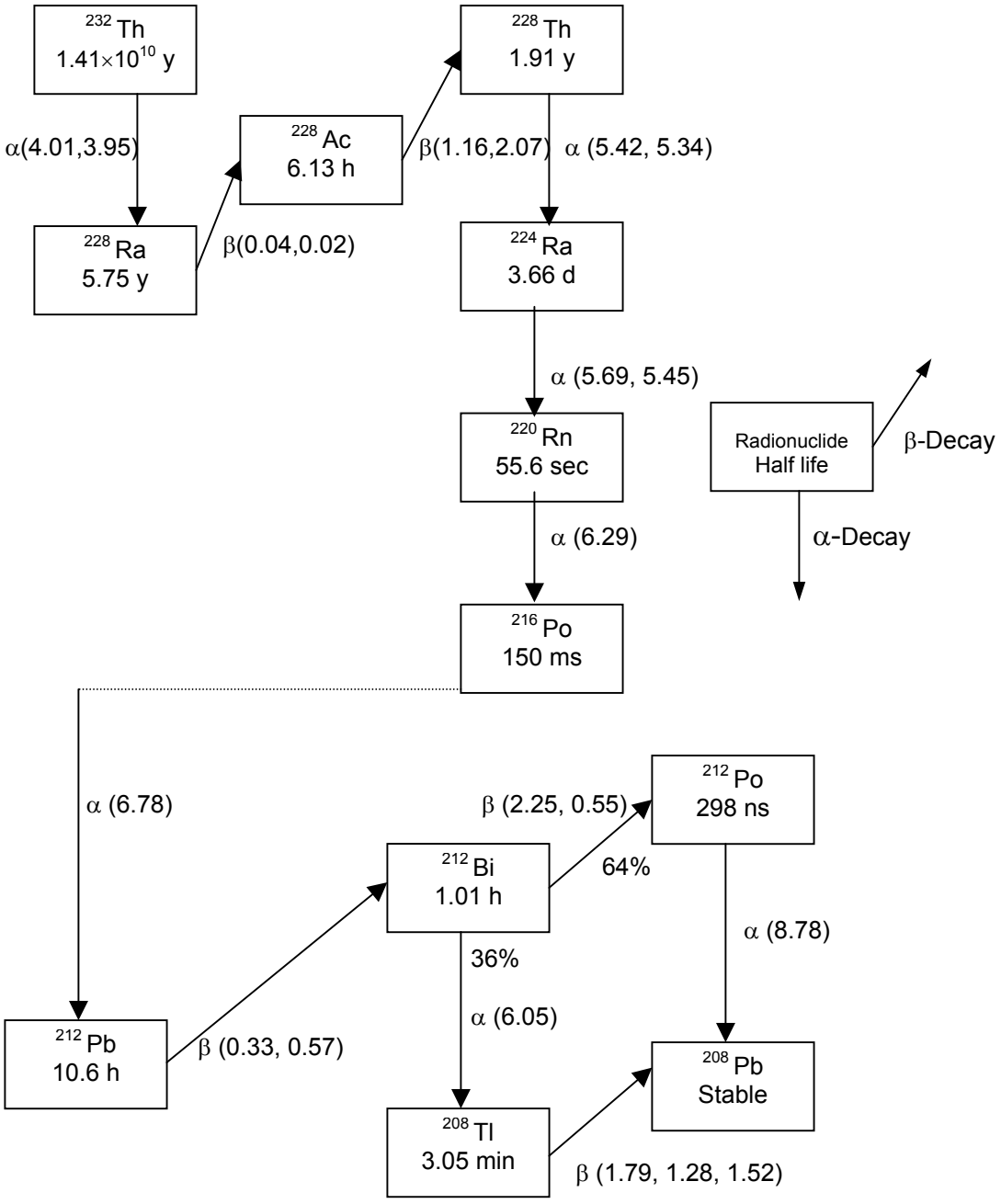

Figure 2.2 Schematic representation of the ^{232}Th decay series, including ^{220}Rn as well as its decay products. The arrows pointing downwards, indicate alpha decay whereas the diagonal arrows indicate beta decay. Alpha and beta energies are given in brackets in MeV [Ner88].

2.3 Characteristics of Soil

2.3.1 Porosity of Soil

There are a few properties of soil that influences the production and transport of radon. One of the properties is the porosity of the soil. It is defined as the ratio of the pore volume to the total volume of the soil. It gives a measure of the storage capacity of the material. According to Nazaroff et al., there are 2 very important components; the textural pore space and the structural pore space [Naz88]. The textural pore space is referred to as the result of random packing of the soil particles whereas the structural pore space is evident in well-aggravated soils. Common porosity values for uniformly sized particle grains fluctuate between 0.25 – 0.5, whereas poorly sorted soils, with a wide variety of grain sizes, possess a porosity value of about 0.3. Van der Spoel gave a very concise definition of porosity in his doctorate thesis [Spo98a]. Using the "Representative Elementary soil Volume" (REV); denoted as δV and expressed as follows

$$\delta V = \delta V_s + \delta V_w + \delta V_a \tag{2.11}$$

where δV_s , δV_w and δV_a make up the sum of the REV as the volume component of the solid, water and air respectively. Since porosity involves the volume of the pore space $\delta V_p = \delta V - \delta V_s = \delta V_w + \delta V_a$, the different porosities are

$$\varepsilon = \frac{\delta V_p}{\delta V}, \tag{2.12}$$

$$\varepsilon_a = \frac{\delta V_a}{\delta V}, \tag{2.13}$$

$$\varepsilon_w = \frac{\delta V_w}{\delta V}, \tag{2.14}$$

where ε is the porosity, ε_a and ε_w is the air-filled and water-filled porosities respectively.

2.3.2 Grain-Size Distribution

Soil samples usually consist of a distribution of grain-sizes. This distribution makes up the soil texture and structure which is integral to radon transport. Soils have been classified in major divisions, such as sand, silt or clay. Typical particle sizes for the major divisions are; sand with a typical range of about 60 – 2000 μm, silt with a range of 2 – 60 μm and clays being that of less than 2 μm [Naz88]. Soil types form in different situations. Larger particles are formed by the physical processes of mechanical weathering, whereas the soil formation for clays are determined by chemical processes. Clays and other metals, together with carbonates often form complexes with uranium and radium which leads to the distributions of radionuclides in the soil [Sch94]. Changes in the grain-size distributions and the control of the extent thereof, together with the presence of grain cements, are due to the redistribution of the earlier mentioned complexes that formed. This would change the permeability of the soil.

The permeability of the soil is defined as how readily something, a gas in this case, would flow through the soil. Soil permeability is determined by the number, the size and degree of interconnection of the pore spaces. Figures 2.3 and 2.4 give a graphical representation of how particles with certain grain-sizes can be arranged. The grains are represented as round in the sketches to illustrate the packing of the aggregates and hence, the control of the permeability. Usually, they have a much more “blocky” appearance than round. The packing of the material in Fig. 2.3, allows for a higher permeability, since the pore space is larger. This is typical for coarse-grained particles. On the other hand, the soil shown Fig 2.4 allow for a lower permeability for the gas to flow, because of the more closely packed particles which leave little

pore space in the interstices of the poorly sorted material. Relating the grain-sizes with the radon emanation coefficient, Markkanen and Arvela found that

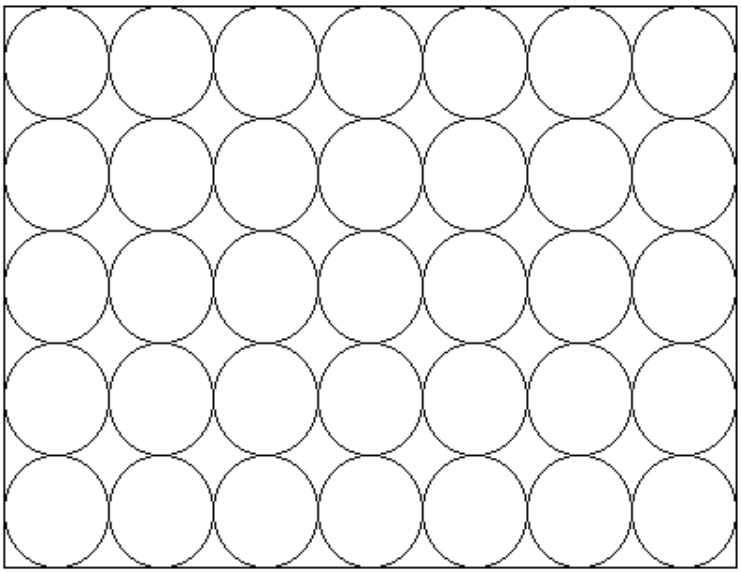

Figure 2.3 Mineral grains with similar diameters, with what is called an open packing arrangement. It allows for higher permeability [Sch94].

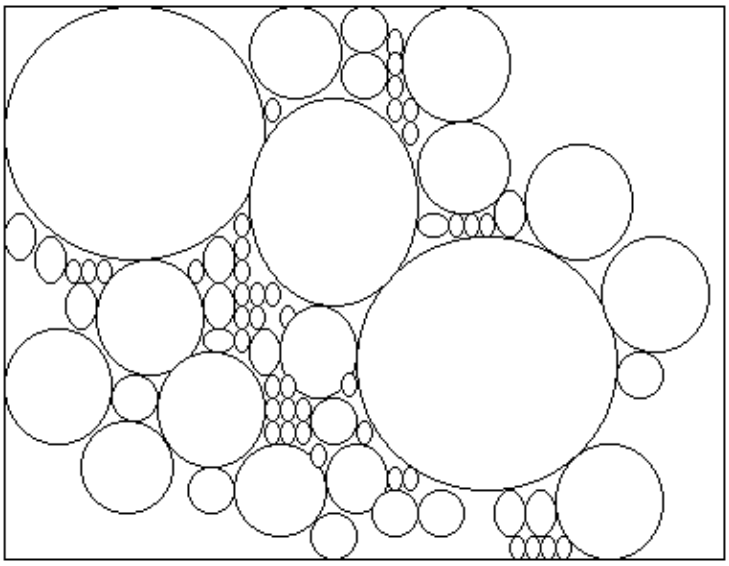

Figure 2.4 Mineral grains packed in a much more poorly sorted manner with a wide variety of grain-sizes, smaller grains in between the larger ones. It allows for lower permeability [Sch94].

radon emanation (the release of radon into pore space, see section 2.4.2) decreases with increasing grain-sizes [Mar92].

2.3.3 Moisture Content

The interstices between soil particles can be filled with air, gas (methane, radon, etc) or may be filled with water or a combination of water and air. The fraction of the volume that is filled with water between the grains is called the moisture content. It is very important, relating to the emanation and transport of radon in soil. The movement of water in soil is usually a fair sign of the permeability to gas movement. Soil with a fair amount of water that is free to move through the pore space, leaves low permeability of gas flow, on the other hand. From this follows that if the soil is much dryer, the permeability for the gas would be higher, and the wet soil, much lower.

The emanation of radon in the pore space of the soil is enhanced in the presence of low to moderate moisture content and rather restricted at higher levels [Sch94]. Moisture content most certainly influences the radon emanation coefficient [Naz88]. Strong and Levin have done a study on uranium ore and tailings [Str82], to show the effects of the moisture content on the radon emanation coefficient. The relative emanation coefficient increases rapidly at first and then slowly increases with the increase of moisture content. Nazaroff concludes that this phenomenon can be explained in the manner that radon has a lower recoil range in water and in case of wet soil, much lower [Naz88].

Radon that enters a pore space filled with some water, would have a very high probability to terminate its recoil in the water and from there, it can be transferred to the air in the pore space that may diffuse to the surface of the

soil. Markkanen et al. found that the effect of water content on the radon emanation to be grain-sized dependent [Mar92]. A range of 10 –15% water content yielded maximum radon emanation for the above mentioned water content, while the grain-size increases. The radon emanation is usually very low for dry materials and eventually reaches a plateau as the moisture content would increase. On the other hand, the radon exhalation from dry materials are usually very low, but reaches a maximum at a certain moisture content and then decreases for higher moisture content [Gra05].

2.4 The Production of Radon in soil

2.4.1 Radium in Soil

Radium (^{226}Ra) is formed in the ^{238}U decay chain as observed in section 2.2.4. Radium always exist only as a trace element in soil, and it co precipitates with elements like magnesium, calcium and barium. Most radium that is exposed to the pore space of the soil will be attached to the grain particle surface, due to the fact that it is efficiently scavenged by magnesium and iron hydroxides as well as organic matter [Sch94]. Weathering processes move radium atoms from within the mineral grains, more to the surface of the grain. This means that once the radium decays to radon, the radon will be liberated much more easily to the pore space. This would directly increase the radon emanation coefficient. Schumann et al. state that, since radium is more inclined to concentrate near or on the surface of the grain particle, together with the fact that most soils have water in between the pores, about 10 – 50% of all the radon atoms that are produced, will leave the solid grain and end up in the pore volume of the soil [Sch94].

Radium content is typically measured in Bq/kg, which is the activity

concentration per unit mass. A radium content of 1 Bq/kg will result in 1 radon atom decay per kilogram per second when the radium and the radon are in secular equilibrium. However, it should also be mentioned that this seldom the case under in situ conditions [Gra05]. The half-life of radium is about 1600 years. Radium is distributed widely in the rocks and soil naturally, and it may or may not be in equilibrium with ^{238}U. Studies of surface soils done in the United States suggest that the typical values for radium range between 10 – 100 Bq/kg for both isotopes; ^{226}Ra and ^{224}Ra [Naz88]. Typical values of radium in soil samples taken from a uranium mine tailings pond in Namibia is of the order of 500$\pm$3 Bq/kg whereas values for the ^{238}U and ^{232}Th are 6500 and 2100 Bq/kg respectively [Ste92].

The average radium activity concentration found by Lindsay et al [Lin04] in a study measuring the radon release from a gold mine tailings dam, range from 70 – 480 Bq/kg. These values are complemented by a follow up study also on the release of radon on the same dump in a MSc-ARST (Acronym for MSc in Applied Radiation, Science and Technology) thesis which obtained an average value of 310$\pm$70 Bq/kg [Mot03]. In both studies mentioned above, the radium content was measured by gamma-ray spectroscopy. As the name suggests, γ-rays that are emitted from the relevant radionuclide are used to determine the activity concentrations.

The analyses are done with a high energy – resolution hyper pure germanium (HPGe) detector. This same technique will also be used to determine the radium content for purposes of this thesis and gamma-ray spectroscopy will also be briefly discussed.

2.4.2 Radon Emanation Coefficient

Radon emanation is caused by direct recoil, due to the emission of an α particle, when the ^{226}Ra nucleus decays. In soil, rocks, building material or anything that contains radium, a radon emanation coefficient is associated with the material, since the radon emanation coefficient gives an indication of the fraction of the produced radon atoms that leave the material itself. The material in this case being gold mine tailings. It is also called the emanating power, emanation fraction or the radon escape-to-production ratio. It has no dimensions and is represented by means of a fraction or as a percentage. Once the radon enters the pore space, the mobility of the ^{222}Rn atoms depend on transport mechanisms like diffusion and advection. The process of diffusion is possible due to concentration gradients of radon whereas with advection, pressure gradients in the soil are the driving force. Radon atoms have a typical recoiling range of about 20 – 70 nm in the host mineral grain, which is dependent on the makeup and density of the grain [Ald94].

Nazaroff et al. describe three divisions in to which the emanation coefficient can be divided. The possibilities are; direct recoil, indirect recoil and diffusion. The first possibility is the direct ejection of the radon atom by recoil from alpha emission. Due to the conservation of momentum, when a radium atom decays with about 4.78 MeV, the residual radon nucleus has a recoil energy of 86 keV [Naz88]. If the radium atom was in a certain range of the soil grain surface, then the resulting radon atom can actually leave the grain (provided it is kicked in the outward direction) and enter into the interstitial pore space. This is depicted in one of the scenarios in Fig. 2.5. If the pore space is filled with water, Tanner suggests that there is a possibility that the radon atom will terminate its recoil in the water [Tan80][Naz88]. The radon atom is then free to diffuse from the water to the soil gas or be transported by it [Fle97].

The second possibility that is plausible is if the radon atom recoils free from the host grain and the interstitial space only contains soil gas. The radon atom might enter the neighbouring grain and terminate its recoil there. The atoms that penetrated the grain can now more freely migrate out of this new pocket to enter the pore space. This is possible, since the created pocket is a result of the radiation damage when the radon atom entered it. The diffusion possibility refers to those radon atoms that are formed further away from the grain surface but then diffuses to the surface. They begin and end their recoil in the same grain (Fig. 2.5 on the next page).

Radon can emanate more easily from a material that is more porous [Åke97]. Emanation from an uncrushed rock, relative to its radium content is low, whereas emanation relative to activity concentrations is larger from a coarse grained granite as an example. It follows from this that radon emanation would increase as a rock is crushed (as in the case of tailings dams) or disintegrates through weathering processes. This would increase the chances of radon emanation for individual mineral grains. It is for this same reason that rocks have lower radon emanation coefficients than soil.

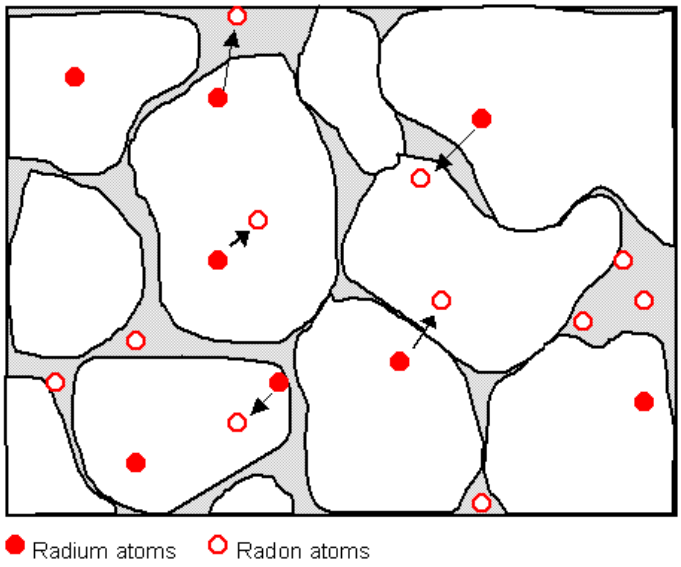

Figure 2.5 Representation of an enlarged section of pore space and soil mineral grains (larger white areas). It also depicts the radium and radon atoms that might be embedded in the grain. The arrows pointing from the radium atoms indicate the recoil direction of the radon atom. The alpha particle from the decay will be propelled in the opposite direction. The representation of the atoms greatly exaggerates the atomic dimensions (Modified after Tanner, 1980).

Chapter 3

Diffusion of Radon in and from a Gold Mine Tailings Dam

3.1 Introduction

In this chapter, a mathematical formulation that describes the radon activity concentration of soil in a mine dump will be derived and certain aspects of it will be discussed. Since the material is porous, the radon levels will be considered inside the pore space that is filled with air. The equation that will be developed, will describe the transport of radon by the process of diffusion only. The equation takes into account the production of new radon as well as the removal thereof, due to the decay of radon during the diffusion process.

Radon diffusion is the result when radon atoms migrate down the concentration gradient. The diffusion is largely described by Fick's Law [Cra75] that connects the concentration gradient to the flux. Later on in this chapter, the parameter that relates the change in radon concentration to the flux of radon atoms; the diffusion coefficient, will be discussed. The diffusion coefficient is medium dependent, i.e. in liquid it would be very much different than in air. This chapter will describe some of the influencing factors surrounding the radon diffusion coefficient as well as the modelling of the radon concentrations by evaluating the time-independent radon diffusion equation. The differences in the radon concentrations brought about by the varying diffusion lengths will also be highlighted in demonstrating a radon depth profile for this specific mine dump.

3.2 Radon Diffusion Coefficient

Random movement of radon atoms in the soil air space result in the migration of radon atoms along the concentration gradient. This is known as diffusion on a molecular basis. As stated in the introduction, the concentration gradient and the flux of the radon atoms can be linked by a diffusion coefficient (D) as described by Fick's Law [Cra75]

$$J_b = -D_b \frac{\partial C}{\partial z} \tag{3.1}$$

or

$$J_e = -D_e \frac{\partial C}{\partial z} \tag{3.2}$$

where J is the activity flux density measured in Bq/m^2s and z is the one-dimensional direction into the mine dump soil. The negative sign in front of the diffusion coefficients arises from the fact that the diffusion occurs in the opposite direction of the increasing concentration. In equations (3.1) and (3.2), different diffusion coefficients are listed as D_b and D_e respectively. Nazaroff et al. distinguish the 2 coefficients by explaining D_b as the bulk diffusion coefficient and D_e as the effective diffusion coefficient. The bulk diffusion coefficient; D_b, relates the interstitial concentration of radon to the flux density across a geometric area, J_b, whereas the effective diffusion coefficient relates the interstitial concentration to the flux density across the pore area, J_e [Naz88]. The most commonly used coefficient is D_e.

The above mentioned coefficients are connected in the following way

$$D_b = \varepsilon D_e \tag{3.3}$$

where ε is the total soil porosity. Typical values for the effective diffusion coefficient for soil with relatively low moisture content, is of the order of 10^{-6} m^2/s. The diffusion coefficient for radon in air is about 1.2×10^{-5} m^2/s. There are numerous factors that influence the diffusion coefficient in a porous

medium like soil; the structure of the pore, the diffusing species, the amount of fluid in the pore space, etc.

3.3 Mathematical Description of Radon Transport in Soil

3.3.1 Boundary Conditions

In this section, an equation that describes the radon activity concentration with respect to the depth of the mine dump will be derived. However, before one does that, there are boundary conditions that need to be stated before derivation. The mine dump soil is considered the radon source as stated earlier. Let us assume that the soil is uniform and that the problem can be approximated as one-dimensional, with the z-axis originating at the surface of the soil and increasing downwards. The radon concentration at the surface of the soil is C_0, whereas the radon concentration tends to a maximum constant value C_{max}, deeper underground. The concentration at the surface is much less than that of C_{max}. With the above assumptions, the boundary conditions can be stated

I. $C \rightarrow C_{max}$ as $z \rightarrow \infty$ (3.4)

II. $C \rightarrow C_0$ as $z \rightarrow 0$. (3.5)

The diffusion equation is a measure of how the concentration of the radon changes with time, but in this system, a steady state is considered, i.e.

$$\frac{\partial C}{\partial t} = 0 . \tag{3.6}$$

The medium in this case is the mine dump soil, which is considered semi-infinite, where the surface of the dump is fixed and z increases downwards as depicted in Fig. 3.1.

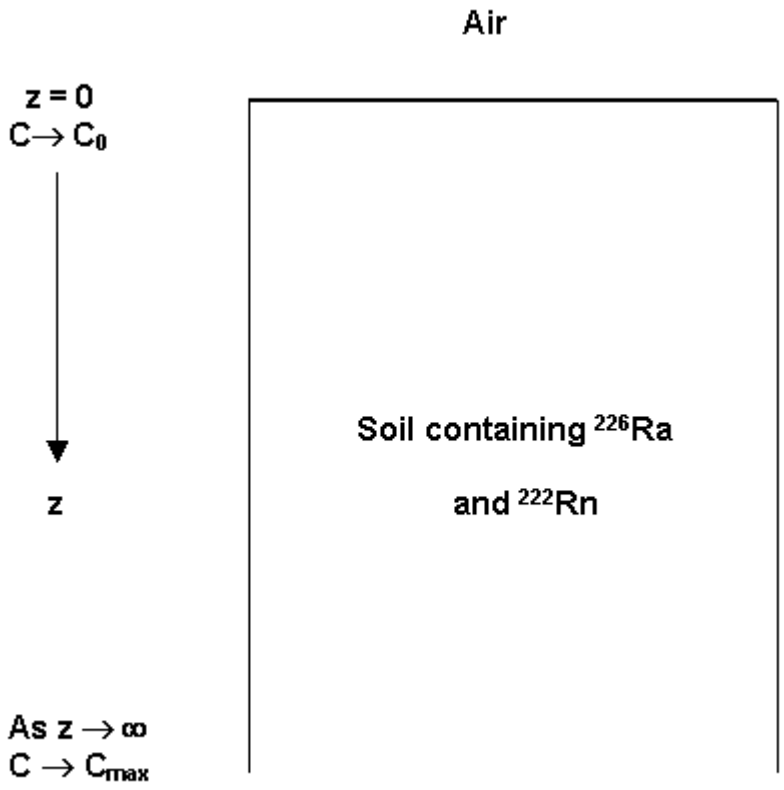

Figure 3.1 Representation of one-dimensional diffusion of radon in a semi-infinite depth of mine dump soil.

3.3.2 Time-Independent Radon Transport

There are two main transport processes that dictate radon release from soil in particular. The 2 processes are diffusion and advection. Diffusion has been previously discussed in section 3.2 and can be better understood in analysing eq. (3.2) that looks at the Flux, J, which is proportional to the radon concentration gradient in the soil.

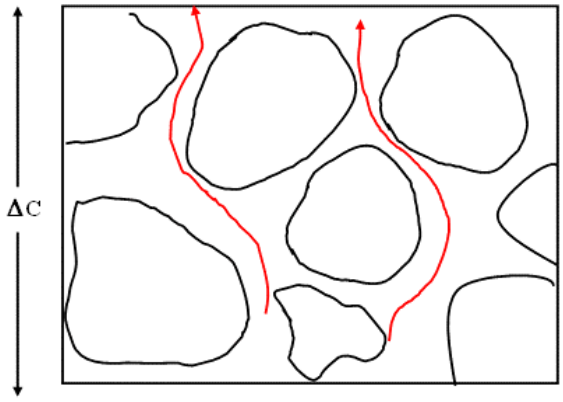

Figure 3.2 Radon transport by means of diffusion processes. The radon concentration gradient causes the movement of radon atoms towards the surface of the mine dump (Modified after van der Pal, 2003).

On the other hand, advective transport of radon in a porous medium is due to the flow of the air in the pore space containing the radon. This is primarily caused by pressure differences and it is believed to be the most important driving force of radon atoms from the soil underneath certain houses. The radon is released into what is referred to as a crawl space of the house, which can disperse further into the house [Pal03].

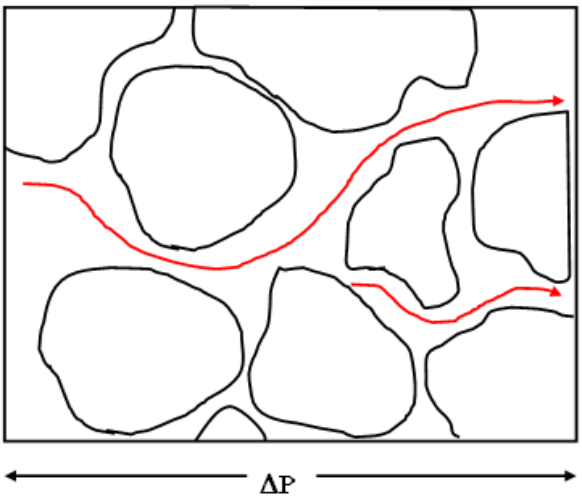

Figure 3.3 Schematic of advective transport of radon atoms. The process of advection is caused by the flow of air in a porous medium like soil. Advective transport is the most important driving force of radon atoms from the soil underneath certain buildings into the crawl spaces and available to disperse into the rooms [Pal03].

The one-dimensional diffusion equation for the proposed model can be written in the following way [Cra75]

$$\frac{\partial C}{\partial t} = D_e \frac{\partial^2 C}{\partial z^2} - \lambda C + S \tag{3.7}$$

with $\frac{\partial C}{\partial t}$ being the change in the radon concentration in the pore space of the soil with respect to time, i.e. the rate of change of radon concentration. The symbol λ refers to the decay constant of radon with value of 2.1 x 10^{-6} s^{-1}. D will be used to signify D_e for simplicity. S is the creation rate of radon per unit bulk volume, measured in Bq/m^3s. The transport equation above is true, when the only transport mechanism is diffusion and when the water content is negligible. Since a steady state is assumed, there is no change in the concentration relative to time. The transport of radon via pressure differences may also contribute a parameter that is derived from Darcy's Law [Ner84]

$$\vec{v} = -\frac{k}{\mu_a} \vec{\nabla} P_a \tag{3.8}$$

where $\vec{v}$ = fluid flow per unit cross section ($m^3m^{-2}s^{-1}$)

k = intrinsic permeability of the soil (m^2)

μ_a = dynamic viscosity of air (Pa.s)

P_a = air pressure (Pa).

Previous studies done by van der Spoel et al. [Spo98b] and Nero et al. [Ner84], found that the small pressure changes in the medium considered, do have an effect on the radon release. In the rest of this section, a one-dimensional numerical model will be derived only considering the transport process of diffusion. This specific modelling calculations is referred to as a classic description, in which constant diffusivity is assumed. Neglecting the pressure term from eq. (3.7) is partly also supported by van der Spoel's findings where the steady state and de-pressurised conditions can be used

for analyses of the 1-dimensional model [Spo98b]. Another reason for neglecting the advection transport of radon, is because of the complexity of the derivation in the model.

Equation 3.7 becomes the following when applying eq. (3.6)

$$D\frac{\partial^2 C}{\partial z^2} - \lambda C + S = 0\,. \tag{3.9}$$

In eq. (3.9), the first term refers to the loss of radon atoms through the process of diffusion, the second term referring to the loss of radon atoms due to radioactive decay and S refers to the creation rate of radon.

Solving eq. (3.9) with the boundary conditions stipulated in section 3.3.1, we can rewrite the second order differential equation as

$$\frac{d^2 C}{dz^2} - \frac{\lambda}{D}C + \frac{S}{D} = 0 \tag{3.10}$$

$$\frac{d^2 C}{dz^2} - \frac{\lambda}{D}C = -\frac{S}{D} \tag{3.11}$$

If we want to solve eq. (3.11), we must first equate it to zero, to get it in a familiar way

$$C = k_1 e^{\sqrt{\frac{\lambda}{D}}z} + k_2 e^{-\sqrt{\frac{\lambda}{D}}z} + k_3 \tag{3.12}$$

The constant k_3 can be obtained by using *particular solutions*, which leads to

$$k_3 = \frac{S}{\lambda} \tag{3.13}$$

So, eq. (3.12) becomes

$$C = k_1 e^{\sqrt{\frac{\lambda}{D}z}} + k_2 e^{-\sqrt{\frac{\lambda}{D}z}} + \frac{S}{\lambda}\,. \tag{3.14}$$

Equation (3.12) is the solution of the homogeneous equation and the general solution is the sum of the homogeneous solution and a particular solution. Now, applying the 1st boundary condition, it is clear that $k_1 = 0$, and the following is obtained

$$C(z) = k_2 e^{-\sqrt{\frac{\lambda}{D}}z} + \frac{S}{\lambda} \tag{3.15}$$

as $z \to \infty$ and the 1st term must be zero otherwise the solution blows up for large z. What we are left with at large z is

$$C_{\max} = \frac{S}{\lambda}. \tag{3.16}$$

The value of C_{max} will be constant deeper into the mine dump as can be observed in eq. (3.16). The reason why C_{max} will be constant, is since no radon is escaping to the surface from deep under, the ^{222}Rn and ^{226}Ra will be in equilibrium. S is termed the production rate of radon (in the pore space) in the diffusion equation or the creation rate as stated earlier, due to the emanation of radon in the soil and is given by [Ald94][Gad95] (See Appendix C)

$$S = \frac{\eta \rho_s \lambda A_{Ra} (1 - \varepsilon)}{\varepsilon} \tag{3.17}$$

where η = radon emanation coefficient

ρ_s = specific density of the soil (kg/m^3)

λ = radon decay constant (2.1 x 10^{-6}s^{-1})

A_{Ra} = radium content (Bq/kg)

ε = porosity of the soil.

Applying the second boundary condition ($C\big|_{z=0} = C_0$) to eq. (3.14), it gives

$$C_0 = k_2 e^{-\sqrt{\frac{\lambda}{D}}z} + \frac{S}{\lambda}$$

$$\Rightarrow \quad C_0 = k_2 + \frac{S}{\lambda}$$

$$\Rightarrow \quad k_2 = C_0 - C_{\max} \tag{3.18}$$

Substituting eq. (3.18) back into eq. (3.14), the final relation can be obtained for the concentration of radon with changing z

$$C(z) = (C_0 - C_{\max}) e^{-\sqrt{\frac{\lambda}{D}}z} + C_{\max}$$

$$\Rightarrow \quad C(z) = C_{\max}(1 - e^{-\sqrt{\frac{\lambda}{D}}z}) + C_0 e^{-\sqrt{\frac{\lambda}{D}}z}$$

$$\Rightarrow \quad C(z) = C_{\max}(1 - e^{-\frac{z}{l}}) + C_0 e^{-\frac{z}{l}} \tag{3.19}$$

with

$$l = \sqrt{\frac{D}{\lambda}} \tag{3.20}$$

and l is referred to as the diffusion length of the radon in soil. Moreover, it can be defined as the average distance traveled by radon atoms in a medium like soil or building materials and can also be seen as the order of magnitude of the projected path length for radon atoms before they decay. Søgaard-Hansen et al. found diffusion lengths of the order of 1.66m for fine sand as well as 1.9m for gravel [Søg87]. They also investigated the diffusion length with respect to clay samples, and they found a considerably smaller diffusion length of 0.87cm. However, it has to be noted that the samples investigated, were water-saturated clay samples.

Chapter 4

Experimental Methods for Measuring Radon and the Radon Emanation Coefficient

4.1 Introduction to Radon Detection

In this chapter, we look at two different methods to measure the radon activity concentration. The first measurement technique is by means of integrative, passive radon sampling, and the second method, by means of continuous active radon sampling. The first method is considered passive, and requires no electrical power as in the case of the continuous radon monitor. The passive integrative radon detector used in this work, uses electret technology to give the average radon concentration during the measurement period [Kot88]. The second device is a continuous radon monitor, which can be used to make multiple readings over a given period. The two techniques differ considerably and will be used to complete different tasks in measuring the factors that affect diffusion of radon.

There are several measuring devices to measure radon levels. These include alpha track detectors, activated charcoal adsorption devices and the AlphaGUARD monitor. The alpha track detector is constructed in such a way that a thin piece of plastic or film is mounted on the inside of the detector. The detector allows for radon to diffuse into the device via a filtered covered opening. The purpose of the filter is to keep dust and radon decay products out. Another function of it is for structural support for the detector housing.

Radon eventually decays in the detector and the emitted alpha particles hit the film and the radiation damage causes a track on the film. The immediate radon decay products may also give off an alpha particle on decay, and hence, leave a track on the plastic. Diffusion barriers are usually constructed to measure the thoron and radon track density separately. The films are then placed in a caustic solution, which enhance the tracks left on the plastic and these tracks can then be counted via an automated system. The number of tracks on the film would give an indication of the radon concentration, provided a few conversion factors are used from the calibration process [EPA92]. A drawback to using track detectors arises when measuring high radon concentrations that cause a high density of tracks per unit area on the film [Ger04].

Activated charcoal devices, as the name suggest, utilises granular-activated carbon to analyse the radon potential. The charcoal is usually kept in containers with a diameter of about 10 cm to 2.5 cm [Geo84]. The top of the canister is covered with a screen for radon to diffuse into the canister and get adsorbed by the charcoal. After the exposure period, the container is sealed and the charcoal is analysed by using a HPGe gamma ray detector to detect the radon decay products [Ger04]. Correction factors also need to be used to calculate the final radon level [EPA92]. The charcoal canisters are usually used for short-term measurements, i.e. from 24 hours to about 7 days. There are a few drawbacks to using charcoal devices, but the most prominent one is the saturation of charcoal due to water adsorption [Ger04].

In this work a different passive method based on electrets will be used. This technique will be discussed in section 4.3. The AlphaGUARD radon monitor on the other hand, is an example of an active electronic device that uses an ionisation chamber that allows for detection through alpha spectroscopy. It

has the added option to pump air into a 0.56-liter cell or by means of diffusion. The two common isotopes of radon, i.e. ^{222}Rn (Fig.2.1) and ^{220}Rn (Fig. 2.2) can be identified through their respective energies from the alpha decays [Swa04]. The signal arising from the alpha detection is then filtered and then converted to a digital output that can be readily processed with the AlphaGUARD or relayed to a PC via a RS-232 cable. It can be used for radon exhalation, radon soil-gas, indoor, outdoor, in mining environments and in water storage radon measurements. An alternate continuous Rn monitor, the RAD7 will be used in this work.

Continuous monitors are very useful in measuring the radon soil gas concentration with depth by means of a probe setup, whereas the passive detector is used to measure the radon emanation coefficient for the soil type considered. The determination of the final value of the emanation coefficient is a combination of the radon emanating ^{226}Ra concentration (RnERaC) from soil as well as the ^{226}Ra content (A_{Ra}) that can be obtained by quantitative analysis. The latter analysis includes gamma-ray spectroscopy by a Hyper Pure Germanium detector (HPGe). An intercomparison will be presented on the modelled radon depth concentrations with varied diffusion lengths, together with actual measurements taken on the mine dump with the continuous radon monitor.

4.2 Durridge RAD7™Continuous Radon Monitor

4.2.1 Continuous Radon Monitors

The RAD7 is a true, real-time continuous radon monitor [Hay03]. This means that a varied radon concentration level can be observed during a measurement period. This is very helpful, in the sense that one can

investigate the factors influencing the radon concentration with time. The factors may include temperature changes, wind speeds, relative humidity and may even give insight into air movements in a room.

Figure 4.1 The Durridge RAD7™ electronic continuous radon monitor with a HP printer mounted for immediate printing of results.

Several types of continuous radon monitors are being sold today, ranging from stationary devices to portable detection devices like the *RAD7™. The portability of the device increases its versatility, since not only can one take measurements at a specific point, but it can also be used to identify entry points of radon into a room, via cracks or fissures. The common term is called ‘sniffing’ for radon, which is useful for mitigating purposes.

Continuous radon monitors work on the principle of particle detection. As observed in Fig. 2.1, there are several radionuclides in the ^{238}U decay series

*RAD7™ is a registered trademark and manufactured by Durridge Company Inc., 7 Railroad Ave., Suite D., PO Box 71, MA 01730, USA.

that decay via alpha radiation and can be easily detected using an α-detector. There are three general types of alpha particle detectors that are used to measure radon, namely

i) Solid state alpha detectors,
ii) Ionisation chambers and
iii) Scintillation cells.

The RAD7 falls in the first category since the detector consists of a semiconductor material. This will be explained in the next subsection. The RAD7 possesses a periodic-fill cell. The cell is filled with air by means of a small pump that draws air into the cell once during each pre-selected time interval. In this defined cell, the radon or the ^{218}Po may decay, and the decays are counted and the cycle repeated. In the second type of detector listed above, radon from the ambient air is allowed to diffuse into an ionisation chamber where the alpha particles from the decay process ionise the air, and the bursts of ions are recorded as individual electrical pulses for each decay by the electronics of the monitor.

The third type of detector utilises scintillation cells. The radon is sampled by means of a pump through a filter. The purpose of the filter is to remove radon decay products as well as dust particles. The radon decay inside the scintillation cells, and the progeny plate out on the interior surface of the cells [EPA92]. The alpha radiation from the radon decay or that of the decay products, strike the coating of the scintillation cell. The subsequent scintillations are detected by a photomultiplier tube (PMT), which generates electrical pulses in turn, which are then processed by the detector electronics.

4.2.2 RAD7 Solid State Detector

The RAD7 radon detector uses a solid state detector. This alpha detector is a silicon ion-implanted detector. The semiconductor material converts the alpha radiation from the decay of the radionuclide (e.g. ^{218}Po or ^{214}Po) into an electrical signal. One advantage of a solid state detector in radon or radon progeny detection is the fact that it can electronically determine the energy associated with the incoming alpha particle. In this way, the specific radionuclide can be identified, ^{218}Po with an alpha radiation of 6.00 MeV or ^{214}Po with an energy of 7.69 MeV.

The RAD7 possesses an internal sample cell of about 0.7 liter and has a hemispherical shape as can be observed in Fig. 4.2. The inside of the hemisphere is coated with an electrical conductor and a high voltage power supply charges the inside of the conductor to a potential of about 2000-2500 Volts relative to the detector. This creates an electrical field throughout the cell. The electrical field propels the positively charged particles onto the detector in the periodic-fill cell. A decaying ^{222}Rn atom within the cell leaves behind a positively charged ^{218}Po, which is accelerated onto the detector and sticks to it. The ^{218}Po nucleus has a relatively short half-life and when it decays, it will have a 50% chance [Dur00] of entering the detector where it will produce an electrical signal, and the energy of the alpha particle can be identified.

The electrical signal recorded from the decay of the radionuclide is then amplified, filtered and then sorted according to its strength. Different modes of functionality of the RAD7 allow for detection of radon from the ^{218}Po signal, but it can also determine the thoron (^{220}Rn) concentration from the ^{216}Po signal. The ^{218}Po and ^{216}Po signals arise from the 6.00 and 6.78 MeV alpha

decays respectively and the alpha energies from the other decay products are ignored. Thoron is formed in the ^{232}Th decay series (Fig 2.2). The subsequent nuclei from further decay include beta emitters but the RAD7 device is almost completely insensitive to beta decay. The RAD7 determines the radon concentration by measuring the radioactivity of decay products.

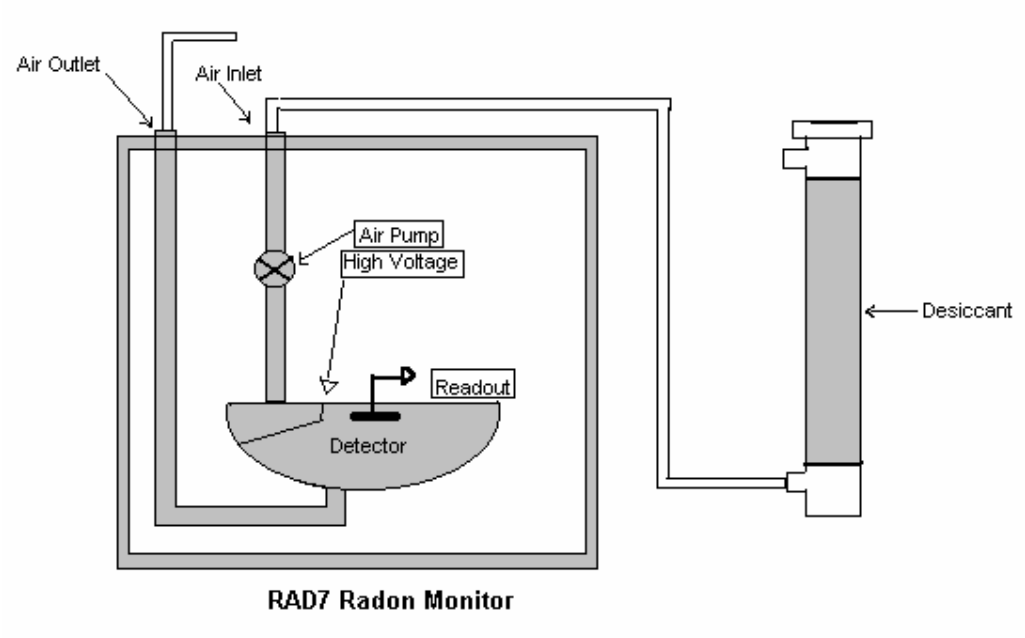

Figure 4.2 Schematic of the RAD7. Special emphasis is put on the hemispherical shaped periodic-fill cell, the high voltage power supply inside the detector as well as the air pump that samples the air to be analysed.

The detector produces a spectrum that will be explained in the next subsection. A very important feature of the spectrum is the absence of the 5.49 MeV peak in the spectrum since ^{222}Rn decays in the air in the cell of the detector and not on the surface or close to the detector. The function of the desiccant in Fig. 4.2 is to adsorb any moisture that was pumped into the tubing to keep the air relatively dry. However, the radon might also get adsorbed on the desiccant granules [Dur00]. This becomes a problem at very high radon concentrations, in which case the RAD7 should be purged.

4.2.3 RAD7™ Spectrum Analysis

The electrical signal produced in the detector due to alpha radiation, is amplified and conditioned by the electronic circuitry of the detector, but also converted to digital form. The RAD7 possesses a microprocessor that receives the signal and stores it in the detector's memory. The signal that is stored is associated with the decay of a specific radionuclide and in the process of accumulating many of these signals, a spectrum can be formed.

The spectrum of the RAD7 can allow for energies from 0 – 10 MeV. Specific interest is shown in the 6 – 9 MeV region, since most of the radon and thoron decay products produce alpha particles in that range. The spectrum is divided into 200 channels that correspond to 50 keV (0.05MeV) per channel. Ideally, in the above spectrum, the 6.00 MeV alpha peak would only be a needle spike as represented in Fig. 4.3, but this is not the case with the RAD7 because of the electronic noise in the detector as well as the amplifier. Another cause for the broadened peaks is the fact that some of the alpha particles enter the detector at a small angle [Dur00]. An increase in the temperature also causes electronic noise, and in turn affects the tail of the peaks. The analysis of the spectrum is simplified because the electronics of the RAD7 is manufactured to group the 200 channels into 8 windows. Those windows are listed as A – H in alphabetical order.

Window A covers the energy range of 5.40 – 6.40 MeV, so clearly the alpha particle with energy 6.00 MeV from the ^{218}Po decay will fall in this region. All the counts detected in that region divided by the livetime (duration of the time that it took to collect the data), gives the count rate. This is all stored in the detector memory.

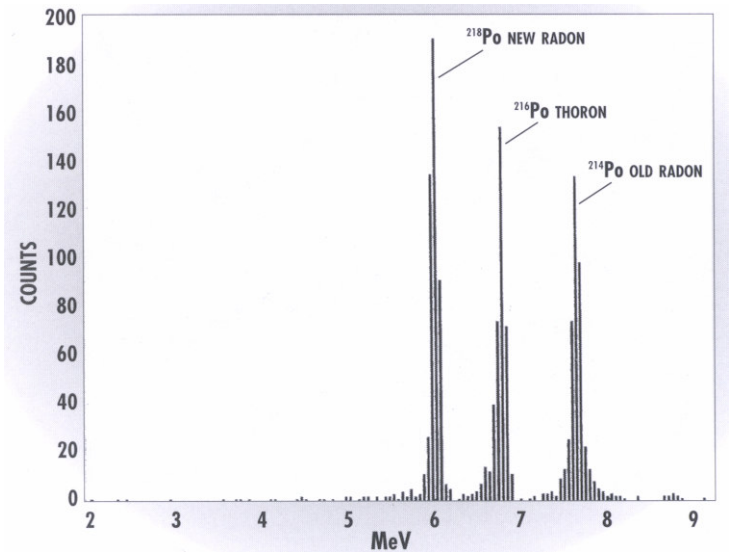

Figure 4.3 An ideal high-resolution alpha energy spectrum [Dur00].

A spectrum is printed by the RAD7 after the run that includes windows A – D. This can be seen in Fig. 4.3. Windows E – H make up the composite window O. Window O is the sum of all the counts arising from energy ranges of windows E – H. The different windows contain:

i) Window A : Total counts from ^{218}Po decay

ii) Window B : Total counts from ^{216}Po decay

iii) Window C : Total counts from ^{214}Po decay

iv) Window D : Total counts from ^{212}Po decay

Window A is used to derive the radon concentration, while windows B and D account for the thoron. The counts from the composite window are due to noise in the system.

4.2.4 Background and Associated Problems

The background reading of the detector is always important, as one can sometime unknowingly underestimate or overestimate the true reading. The manufacturer of the RAD7 radon monitor claims that the RAD7 is unlikely to

be or minimally affected by background [Dur00], but also warns of a number of possible problems.

Radon and thoron decay products are the most likely contributors to affect the background in the RAD7. They cause problems when trying to measure lower radon concentration soon after a high reading. This problem is partly solved since the detector can distinguish their energies. Another problem that is worth noting is ^{210}Pb. It is a deciding factor in most instruments due to the tendency of build-up (long half-life), but this is not a problem with the RAD7, since ^{210}Pb is a beta-emitter. One of the radionuclides following the ^{210}Pb decay (Fig. 2.1) is ^{210}Po, which is an alpha-emitter. This is ignored in the calculation of the final value, because of its energy distinction in the spectrum. Another possible problem found in the analysis of the data in this work might include the setup of the RAD7 for radon soil-gas measurements (subsection 4.2.5). Air might be leaking into the setup even though some precautions are taken to minimise it. The use of *Teflon™ tape is advised by the manufacturer when assembling the apparatus, but the integrity might be questioned in a setup like this. A problem of the same nature arises when inserting the probe into the ground when trying to measure the radon concentration in the soil. The diameter of the probe head is a little bigger than the probe shaft, and upon insertion, a little space is left on the side of the shaft. This is minimised by tapping down the soil into the open space surrounding the shaft to stop the soil-gas from becoming diluted as air might be sucked down the outside of the shaft. This would be the more prevalent at shallower depths and dubious results could be expected.

*Teflon™ is a trademark of the product manufactured by E.I. Du Pont de Numours and Co., Washington, DE 19898, USA.

4.2.5 Radon Soil-Gas Measurements

Radon concentrations at different depths have been measured through several projects [Åke97]. Especially of interest are the radon concentrations in mine tailings from uranium mining. In a mine dump, the radon concentration grows by the process of radon emanation, but processes like decay or diffusion may also remove it. Measuring the radon concentration at different depths would give an indication of the radon available (given a fair diffusion length for radon) to diffuse to the soil surface and out, or by meteorological changes at shallow depths. Åkerblom et al. suggest that taking radon measurements at a depth around about 1meter, since this greatly minimises errors that arise from shallow depths (subsection 4.2.4). Another reason for suggesting depths around 1 meter is that via the process of leaching of the radium and uranium from the top soil, the radon concentration would be more likely to be stable at these depths than at subsoil levels [Åke97].

A research project done by Bigu et al. on the mill tailings of a uranium mine in Canada, at a depth of about 50 cm, a radon concentration of 670 kBq/m^3 was recorded and about 4000 kBq/m^3 was recorded at a depth of 5.70 m [Big84].

4.2.6 Radon Soil-Gas Setup on Kloof Mine Dump

There are a few types of soil-gas monitors that give real-time radon readings. Bigu et al. used the α-Probe 601 [Big84] to complete a radon soil depth profile, whereas the RAD7 will be used to measure the profile of the radon soil-gas in this study. Figure 4.4 shows the RAD7 with the probe. The white

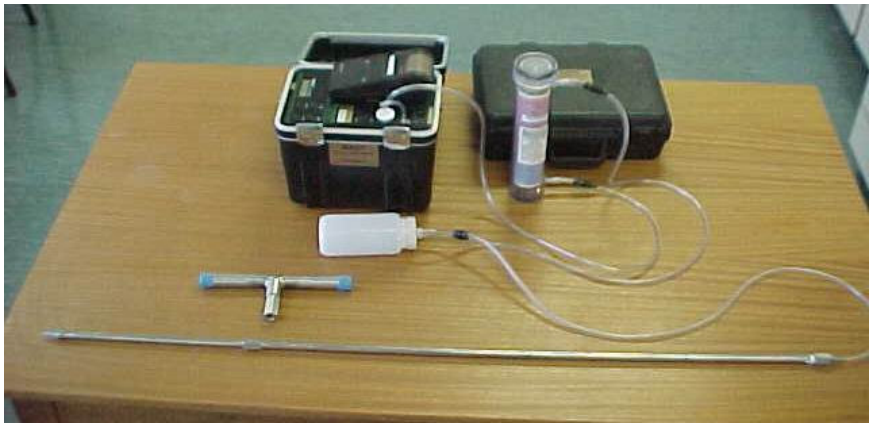

Figure 4.4 The RAD7 soil-gas setup, including the electronic radon monitor and a steel probe and shaft of length about 1.3m.

bottle included in the setup serves as a water trap that condenses moisture onto the surface of the bottle to prevent the desiccant material (upright holder with pink and blue contents) not to lose its moisture absorption ability too quickly. A problem that could arise from using the water trap, is the adsorption of radon onto the inside of the bottle. The purpose of the desiccant material is to ensure that the air pumped into the periodic-fill cell of the RAD7 is relatively dry. The probe tip and shaft are inserted into the mine dump soil by hand (using the cross handle in Fig.4.4) for lower depths. The deeper the probe is inserted into the ground, the more force has to be used. A rubber or slide hammer is then used.

Teflon tape is wound round the screw joints to create a reasonably airtight fit. The tip of the probe is constructed slightly wider than the probe shaft to prevent the sampling points (located just after the probe tip) from clogging up with sand. The design of the tip made it difficult to retract the probe. The mine dump soil, being a bit damp, compresses quickly when trying to pull the tip out. At depths of about 1.3 meters the problem was so persistent that the probe and shaft had to be dug out by spade.

The RAD7 can measure radon via 3 different modes. The mode used for the soil-gas measurements is called the Grab sample protocol. The RAD7 pumps the soil-gas for 5 minutes into the cell of the detector, and then waits for 5 minutes and only then counts for 5 minutes. ^{218}Po has a half-life of 3.05 min and it takes about 3-5 half-lives for the ^{218}Po activity to reach secular equilibrium, hence, in about 9-15 minutes. The decays of the ^{218}Po would then be counted after 10 minutes (5 minutes of pumping plus 5 minutes of waiting), in which time 95% of equilibrium would have been reached [Dur00]. In total, each set of readings includes four 5-minute cycles that in total takes 1 half hour.

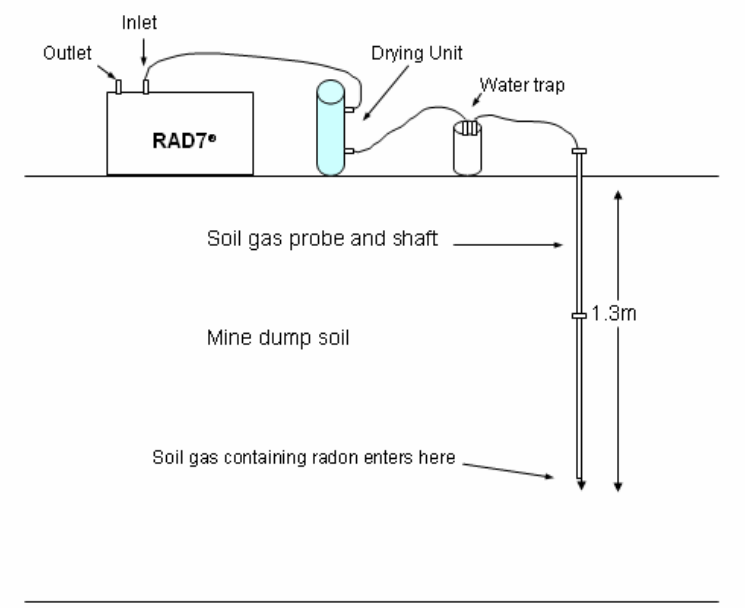

Figure 4.5 Schematic of the RAD7 soil-gas setup as would be seen from the side of the mine dump.

The pump of the detector usually pumps 1L/ min of air by means of the electronic pump inside the RAD7 (Fig.4.2), but is estimated to pump only 0.3 – 0.5 L/min of soil-gas. In pumping 5 minutes at the beginning of each cycle, it removes about 2 – 2.5 L of soil-gas to be counted for radon. The depth of the sampling point is determined by the length of the probe inserted into the

ground taking into consideration the location of the sampling points on the probe shaft. The pump of the RAD7 is switched on beforehand, to purge the water trap with soil-gas as well as to bring the relative humidity inside the instrument to less than 7%. After purging for a few minutes with the probe set at a selected depth, the experiment was started to measure the radon activity at different depths. The sampling was done from shallow to deep. The length of the probe only allowed for depths up to 1.25m. Actual measurements were taken at two different spots on the mine dump. The two points were named M1 and M2 for sampling purposes. The GPS coordinates of the two spots are

i) M1 - 26º 24.797' South Latitude
27º 37.111' East Longitude

ii) M2 - 26º 24.802' South Latitude
27º 37.404' East Longitude.

Once the depth profile data was recorded, soil samples were collected at those points to be counted by means of an HPGe γ-detector to get the radium content.

4.3 Radon Measurements Using *E-PERM® Systems

4.3.1 Ion Chambers

The E-PERM (Electret Passive Environmental Radon Monitor) detectors are used widely around the world for measuring radon in air [Kot88]. The E-PERM system is based on electret ion chamber (EIC) technology. It consists of a few components to complete the setup; the first is an ion chamber made of electrically conductive plastic that can be purchased in a variety of shapes.

* E-PERM™ is a registered trademark of the product manufactured by Rad Elec Inc., Frederick, MD 21701

The second part is an electrically charged Teflon® disk called an electret, that can be mounted inside the above-mentioned chamber. The third component to complete the E-PERM system is an electret reader that is needed to measure the surface potential (voltage) of the electret [Rad94]. A common name for the system is an EIC.

There are several detectors available to measure nuclear radiation. One way is to use an electric field to gather ions caused by ionisation radiation [Kra88] and a very simple type of detector that uses this technology is the ionisation chamber. The E-PERM monitoring system is one such example. Gas-filled counters (Geiger counters) are the other very common example that makes use of a cylindrical proportional counter. The current that is induced from the incoming radiation is proportional to the energy of the radiation as well as the activity of the source. This means that if higher radiation is present, more ionisation will occur.

The EIC can measure short-term as well as long-term radon concentrations in air, radon in water and radon emanating from soil. The technology may also be used to measure the radon flux from surfaces and mill tailings [Liv97]. Other advantages of the system include its integrating nature when taking measurements as well as the fact that it is minimally affected by changing temperatures and relative humidity [Kot92a]. This makes it suitable for outdoor environments as well. The E-PERM system was developed primarily for measurements of radon in houses. The detectors have proved to be very accurate and can be used in a glass jar with a calibrated source as a calibration chamber [Col95]. In this work, the glass jar will be used to measure the radon that escapes from a soil sample.

4.3.2 Electret Technology

The electret disks are shown in Fig.4.6 in long-term (black face) and short-term (white face) versions. They are constructed in such a way that the Teflon disk is secured in an electrically conducting plastic holder that helps to screw the electret securely into the ion chamber. The electret is electrically charged, with an initial electret voltage round about 750 Volts. The charged electret is then screwed into a semi-closed detector volume (EIC) so that the electret produces an electrostatic field inside the chamber. The created field is so strong that it can attract ions from inside the chamber onto the disk (field lines depicted in Fig. 4.10). The α-decay of radon and its progeny produces α-particles with 5-7 MeV. This energy is lost by the interaction of the positive α with (mainly) the atomic electrons in the air. The electrons that result from ionisation are attracted to the positive electret and reduce the voltage.

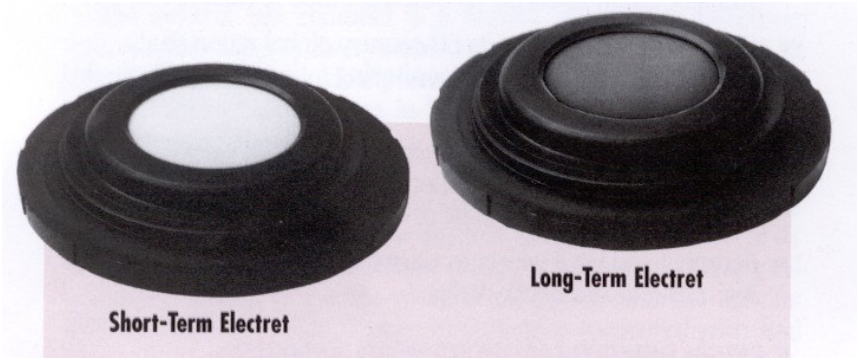

Figure 4.6 Long- and short-term electrets manufactured by Rad Elec Inc.

The change in the charge of the electret over a certain time is related to the integrated radon concentration. This relationship is explained in Appendix A together with factors influencing the final radon concentration. There are 3 types of electrets that are manufactured for different purposes. The 3 types are color coded in blue, green and red and they are manufactured with different thicknesses for their use in long-term (LT) or short-term (ST)

measurements. The blue and green electrets are the more sensitive ones and are used for short-term measurements. The red labeled electrets are less sensitive and are used for long-term measurements. The thicker electrets are the short-term ones with a thickness of 1.542mm and the long-term electrets have a thickness 0.127mm [Kot90]. One of the reasons for the difference in the thickness of the electrets, is to optimize the sensitivity and the range of the E-PERM system. Kotrappa et al. showed that a thicker electret would have a proportionate amount more surface potential than a thinner electret when both electrets have the same charge. It follows from that, that an E-PERM fitted with a thicker electret has higher sensitivity, but with a shorter range. However, higher sensitivity is also a result from a larger volume E-PERM [Kot88].

Electrets are very sensitive devices and may not be touched by hand or any objects, e.g. dust or fibers. The permanently charged disk that serves as a source for the electric field as well as a sensor will lose its voltage once touched and rendered useless. It is for this reason that electrets are covered with a protective cap if not in use. Exposure of electrets to ionising radiation causes a reduction in the surface voltage of the electret and hence an electret reader is necessary to measure the initial and final voltages.

4.3.3 The E-PERM Electret Ion Chambers

There are several electret ion chambers commercially available, but only 2 different volumes will be used for this study. The 3 most commonly available EICs are the “L”, “S” and “H” type of chambers (herein afterwards only referred to as L, S and H chambers). The S chamber has a volume of about 210ml and is used for intermediate short-term measurements for 2 days and more. The L chamber has a volume of about 50ml and is used for long-term measurements. The H chamber is the largest of the 3 volumes at 960ml and

is also the most sensitive to radon [Rad94]. The S and L chambers may be used either with LT or ST electrets, whereas the H chamber may only be used with ST electrets. Figures 4.7 and 4.8 show the different type of chambers.

Figure 4.7 The S chamber E-PERM detector [Rad94].

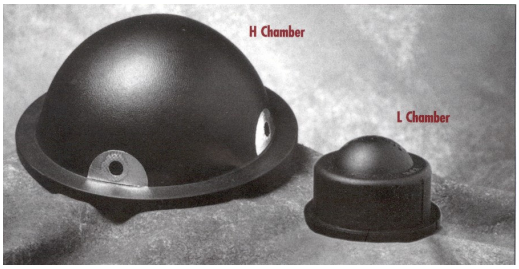

Figure 4.8 The H and L chamber E-PERM configurations [Rad94].

The S chamber has an on/off mechanism that works with a spring-loaded cap to stop or allow air and radon to diffuse into the chamber. Fig. 4.9 shows a schematic of an electret mounted into a S chamber in the on/off position.

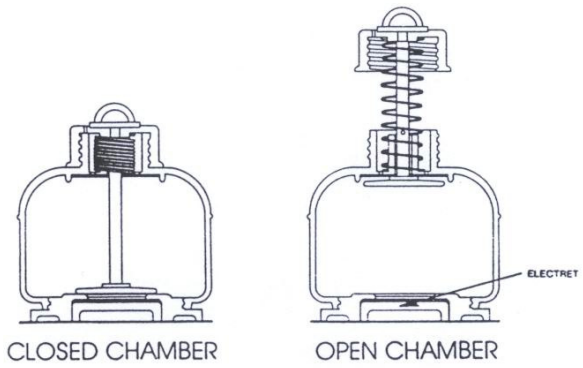

Figure 4.9 Schematic of the S chamber in an on and off position showing the spring mechanism.

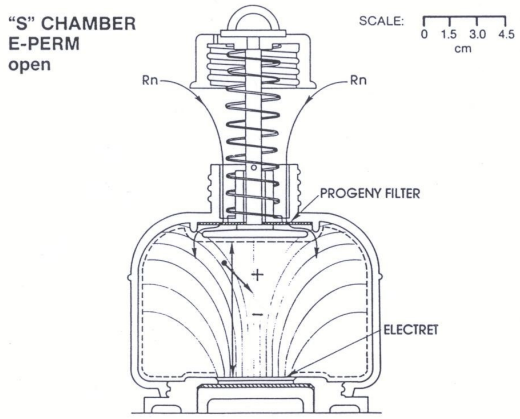

Figure 4.10 Schematic diagram of the S chamber fitted with an electret that causes an electric field inside the chamber and consequently attracts the ions produced from the ioninising radiation to the electret disk [Rad94].

The chambers that will be used in this study are the L and S chambers. They are used to measure the radon emanating ^{226}Ra concentration (RnERaC) from soil samples collected at the gold mine dump in the Gauteng province. The samples were analysed in a leak-tight accumulator jar. The procedure will be discussed in one of the next subsections.

4.3.4 Electret Readers

There are 2 types of electret readers. The 2 types that are commercially sold by Rad Elec Inc. are the SPER-1 (Surface Potential Electret Voltage Reader) and SPER-2 (shown in Fig. 4.11). The SPER readers are used for measuring the surface voltages of the electrets before and after exposure to radon. The change in the surface voltage is a measure of the radon concentration in the E-PERM system during the exposure period. The SPER-1 and -2 technologies are high precision electronic instruments with a non-contact voltmeter. Both the voltage readers are portable with only the SPER-2 reader with an option to connect to power mains.

Figure 4.11 A picture taken of the SPER-2 (left) and SPER-1 (right) electret readers.

The electret is put face down into the circular receptacle on top of the SPER readers. Beneath the electret surface (slight distance separation), there is a shutter-window that can be retracted and released so that the reader may take the surface potential of the electret. The whole procedure is non-destructive so that the electrets may be measured repeatedly without affecting its voltage. The internal electronics of the SPER-1 reader encompasses an ultra-low leakage detector that gives very stable readings [Kot88]. The reader can measure surface potentials up to 1999 Volts and can be precise to ±1 Volt in both the initial and final readings [Rad94]. The SPER-1 reader needs no calibration once received from the manufacturer but voltage response stability checks should be made routinely. The checks are performed with reference electrets. The reference electrets are highly stable electrets with exact voltages that need to be read weekly to monitor the stability of the reader.

The SPER-2 reader is an advanced reader with a built-in microprocessor that handles data storage, retrieval, computation and interfacing thereof. The

reader can also be connected to a computer for data upload. The core essentials of the SPER-2 reader are the same as that of the SPER-1, but with the above-mentioned features added. Both readers were used in this study.

4.4 Radon Emanating ^{226}Ra Concentration (RnERaC) from Mine Dump Soil Samples

The radon emanation is a very important parameter in estimating the radon flux from a gold mine tailings dam [Lin04] or determining the production rate; S of radon as in subsection 3.3. In order to determine the radon emanation coefficient, 2 parameters have to be measured. The first will be discussed in this section and it gives a measure of the radon escaping from ^{226}Ra (RnERaC) bearing soil. The second parameter includes the determination of the radium content (A_{Ra}) in the mine dump soil samples. The radium content will be discussed in the next subsection. The RnERaC method [Rad94] incorporates the E-PERM technology whereas the determination of the A_{Ra} is done using an HPGe γ-ray detector. The final value for the radon emanation coefficient can then be obtained. The ratio of the RnERaC and A_{Ra} gives the radon emanation coefficient (η) in the following way

$$\eta = \frac{RnERaC}{A_{Ra}} . \tag{4.1}$$

The measurement of the RnERaC using the E-PERM's, is a direct method and is reported in Bq/g or Bq/kg and can be calculated by using the following expression derived from Collé et al. [Col95] as well as Kotrappa et al. [Kot94]. Consider an accumulator jar with a volume V_a containing a thin layer of soil with mass G. The ^{222}Rn activity concentration $\overline{C}_{Rn}$ inside the closed jar will grow in according to the following relation

$$\overline{C}_{Rn} = \frac{\eta A_{Ra} G}{V_a}(1 - e^{-\lambda t}) + \overline{C}^{0}_{Rn} e^{-\lambda t} \tag{4.2}$$

where η = radon emanation coefficient

A_{Ra} = Radium activity in Bq/kg

G = mass of the soil sample in grams

V_a = air volume in the accumulator jar in liters

λ = decay constant of radon (0.1813 $days^{-1}$)

$\overline{C}^{0}_{Rn}$ = initial radon concentration in the jar (approximately ≈0Bq/m^3)

t = accumulation time.

The integrated radon activity concentration I_{Rn} from t=0 to t = T_a would then be

$$I_{Rn} = \int_0^{Ta} \overline{C}_{Rn} dt \tag{4.3}$$

$$= \frac{\eta A_{Ra} G}{V_a} \int_0^{Ta} (1 - e^{-\lambda t}) dt$$

$$= \frac{\eta A_{Ra} G}{V_a} \left[T_a - \left(\frac{1}{\lambda} \right) \left(1 - e^{-\lambda T_a} \right) \right]. \tag{4.4}$$

The time-averaged ^{222}Rn activity concentration C_{Rn} (Bq/m^3) from eq. (4.4) is

$$C_{Rn} = \frac{I_{Rn}}{T_a} \tag{4.5}$$

$$= \frac{\eta A_{Ra} G}{V_a} \left[1 - \frac{\left(1 - e^{-\lambda T_a} \right)}{\lambda T_a} \right]. \tag{4.6}$$

Hence

$$\eta = \frac{C_{Rn} V_a}{A_{Ra} G} \left[1 - \frac{\left(1 - e^{-\lambda T_a} \right)}{\lambda T_a} \right]^{-1}. \tag{4.7}$$

Equation (4.1) can be rewritten as the following

$$\text{RnERaC} = \eta * A_{Ra} \tag{4.8}$$

and substituting eq. (4.7) in eq. (4.8) to obtain the following

$$RnERaC = \frac{C_{Rn} V_a}{G} \left[1 - \frac{\left(1 - e^{-\lambda T_a}\right)}{\lambda T_a} \right]^{-1} \tag{4.9}$$

$$RnERaC = \frac{C_{Rn} V_a}{G} K \tag{4.10}$$

where

$$K = \left[1 - \frac{\left(1 - e^{-\lambda T_a}\right)}{\lambda T_a} \right]^{-1} . \tag{4.11}$$

Equation (4.9) is then used to determine the final RnERaC values for the soil samples.

The accumulator jar has a volume of about 4 liters. Each of the E-PERMs used in the jar, decrease this volume and the final answer depends on the air volume (V_A) in the jar. Kotrappa et al. measured the different volumes experimentally for a variety of E-PERMs as well as different quantities inside the jar.

Figure 4.12 Two S-chambers fitted with electrets inside the sealed accumulator jar. The soil sample is contained in the silver dish.

Table 4.1 shows some of the data obtained for the corrected air volumes [Kot94].

Table 4.1 The air volumes inside the accumulator jar when different types and numbers of E-PERMs are used.

E-PERM Configuration	Number of Chambers	Air Volume of Jar ml
SST/SLT	1	3843
SST/SLT	2	3720
LST/LLT	1	3920
LST/LLT	2	3873

Soil samples were collected on the mine dump and about 30 – 40 grams were placed on a small dish (preferably a wide Petri dish) and placed inside a leak tight accumulator jar for a RnERaC measurement (Fig. 4.12). The samples were prepared by drying them in the laboratory for at least a week, before being placed inside the jars. The samples were dried, because at first a lot of condensation were noticed on the inside of the accumulation jar. The humidity inside the jar was a concern at warmer temperatures, since it encourages fungal growth on the electrets [Kot00]. All organic matter and debris were removed from the sample before the measurement would start. The collected mine dump soil samples were processed to get rid of organic matter, like roots, grass and leaves. As expected, very few stones were found in the soil. The S and L chambers were used together with ST electrets in this study. The SST and LLT naming in Table 4.1 refer to a S chamber fitted with a ST electret and a L chamber fitted with a LT electret respectively. The initial voltages (I) on the electrets were recorded and the electrets were screwed into the relevant chambers and sealed inside the jar. The jars loaded with the samples and E-PERMs were then left in a room at constant temperature of about 25°C. The exposure period ranged from 7–30 days depending on the chamber that was used.

Once the exposure period was over, the electrets were collected and careful measurements of the final voltages (F) were taken. The average radon concentration was then calculated using the standard method (see Appendix A). The other data including the mass, exposure time, together with the average radon concentration was used to determine the RnERaC using eq. (4.9).

4.5 Radium Content by HPGe

The ^{226}Ra activity concentration in the samples collected at the gold mine dump were measured using a Hyper Pure Germanium (HPGe) detector. The analysis is based on the gamma-ray spectroscopy method that is used routinely in the Environmental Radioactivity Laboratory (ERL) of iThemba Laboratory for Accelerator Based Sciences (LABS). The setup uses a Canberra γ-ray detector with an efficiency of 45%, a lead castle constructed around the detector and a Marinelli beaker to hold the soil sample for counting. The purpose of the lead castle is to shield the detector from as much background radiation as possible that might originate from cosmic rays, etc. Roots, grass and leaves were evident in the soil because of the rehabilitation process on the tailings dam established to minimise erosion as well as excessive dust blowing from the dump.

The samples were spread out on trays for overnight heating at a constant temperature of 105 ℃. The dried samples were then placed in clean Marinelli beakers with copper lids placed on top of the samples. The lid of the Marinelli was then sealed tightly with a sealant. The samples were then stored in the laboratory for a period of 3 weeks to let the radionuclides reach equilibrium inside the beaker. Once this process has finished, the samples were counted

for 10 hours using the HPGe detector setup at iThemba LABS. In order to calculate the final ^{226}Ra content, secular equilibrium is assumed between the ^{226}Ra and the γ-emitters ^{214}Pb and ^{214}Bi.

The radium content is very important to this study, as it is used to determine the radon emanation coefficient that characterises this specific dumpsite in terms of radon transport. The results of the analysis are also used in γ-ray mapping [Lin04], where the laboratory measurements of collected samples are used for calibration purposes. The other important point that stems from measuring the radium content, is the determination of the creation term of radon; S (section 3.3) in the soil. This leads to the prediction of the maximum radon concentration; C_{max}.

4.6 Methodology for Measuring the Porosity of Kloof Mine Dump Samples in the laboratory

Soil samples collected at the Gold Fields mine dump were sealed in sampling bags and tagged for processing at UWC and iThemba LABS. One of the analyses performed on the soil samples, was the determination of the total soil porosity. The method that was used is a fairly simple one suggested by Conway that investigated a variety of soil types by looking at the effect that changing particle size has on the porosity (ε) of the soil [Con99]. His findings concluded that smaller soil particles allow for a larger total porosity.

The preparation of the Kloof samples was processed to get rid of plant material, animal feces or roots that might influence the porosity value considerably. A total of 50 grams of the soil was weighed and then transferred to a measuring cylinder. The mass as well as the (dry) volume of

the soil was recorded. All of the weighed contents were then transferred to another measuring beaker containing 50cm^3 of tap water. The measuring beaker containing the soil and water was then left to stand for about an hour. The total porosity of the soil was then calculated using the ratio of the volume of the air to the volume occupied by the soil,

$$\text{Total porosity} = \text{Volume of air} / \text{Volume of soil} \tag{4.12}$$

The experiment was repeated several times with soil collected throughout the mine dump. The room temperature was recorded at about 23±1°C. The results are presented in Chapter 5.

4.7 Methodology for Measuring the Specific as well as the Bulk Density of the Mine Dump Soil

The soil samples were also investigated for determination of its specific (ρ_s) and bulk (ρ_b) densities. The specific density of a material is defined as the mass per unit volume. The specific density of the soil is also linked to the bulk density in the following way:

$$\rho_b = \rho_s (1-\varepsilon) \tag{4.13}$$

The bulk density of the soil gives an indication of how much soil would be packed as a whole into a certain volume. The methodology to determine the specific density was derived from the method used by van der Spoel [Spo98a]. The method included using a measuring beaker into which a non-specific mass (M_s) of soil is transferred. The beaker was then filled up to 500cm^3 of tap water with mass (M_w). The specific density can then be calculated using the following relation

$$\frac{M_w}{\rho_w} + \frac{M_s}{\rho_s} = v_f \tag{4.14}$$

where M_w = mass of water added to soil (kg),

M_s = mass of soil investigated (kg),

v_f = measured volume of combined soil and water (cm^3),

ρ_w = density of water at the specific room temperature (kg/m^3) and

ρ_s = specific density of the soil in kg/m^3.

The room temperature was recorded at 22°C and consequently the density of the water is 0.9978 kg/m^3 [Spe03]. The final calculation was then was made using eq. (4.14). The bulk density ρ_b was then calculated using eq. (4.13) together with the porosity (ε). The parameters ρ_b and ρ_s are used to determine the creation rate S of radon in the mine dump soil. Kumar et al. describes the S term as the integrated radon exposure that is measured in Bq/m^3s [Kum03].

Chapter 5

Results and Discussion

5.1 Introduction

All the results from the study on the mine dump as well as the laboratory investigations will be presented in this chapter. This includes the determination of the radon emanation coefficients using 2 types of EIC's (S- and L-chambers) to measure the radon emanating from the radium bearing soil (RnERaC) together with the approximate determination of the uranium content (A_{Ra}) by using an HPGe gamma-ray detector. The actual raw data from the experiments in the laboratory is presented as well as a summary thereof. A one-dimensional mathematical relation was derived in Chapter 3 to predict the radon soil-gas concentration in the dump. The plot of the modelled data is presented, together with a few assumptions, to determine the maximum radon concentration for different diffusion lengths.

The results of the radon soil-gas depth measurements are also presented here, which were measured with the RAD7™ electronic radon detector. Soil samples have been collected close to the surface at the points where depth measurements have been made. An intercomparison between the RAD7 and one-dimensional model will also be discussed. The parameters that govern the output for the modelling of the radon concentration include the porosities, specific and bulk densities of the soil considered. The results for the porosity, specific and bulk densities are also presented. Lastly, the results will be discussed throughout the chapter to show how it impacts other studies that relate on to this one and to also discuss influences on the different parameters.

5.2 Radon Emanation Coefficient Experiments

The radon emanation coefficients for the different soil samples are listed in tables 5.2 and 5.4. Table 5.2 lists the radon emanation results obtained by using the S-chambers suggested in chapter 4. Table 5.4 lists the results obtained from using L-chambers. Different factors to note are the mass of the soil samples, the air volume inside the accumulator jar derived from Table 4.1 (depending on the number of EIC's that were used in the jar). In Tables 5.1 and 5.3, the accumulated radon concentrations are listed for the experiments that were done for different durations. The radon concentration can be calculated using eq. A.1 (Appendix A). The calibration factors for the different setup of EIC's are determined by using equations (A.2) and (A.4) (listed in Appendix A) for an SST and LST setup respectively. The uncertainties in the results are determined using eq. (A.8) in Appendix A.

Radon emanation has an important influence on the radon flux from a gold mine tailings dam [Lin04]. In order to determine the radon emanation coefficient, two parameters have to be measured. The first parameter gives a measure of the radon emanating from ^{226}Ra (RnERaC) of the soil. The RnERaC is determined using eq. (4.9) whereas the factor K in table 5.2 and 5.4 is determined using eq. (4.11). The second parameter includes the determination of the radium activity concentration (A_{Ra}). The RnERaC method [Rad94] incorporates E-PERM technology whereas A_{Ra} is determined using an HPGe γ-ray detector. The radium content is obtained from Table 5.6 that also list the thorium and potassium content. The ratio of the RnERaC and A_{Ra} gives the radon emanation coefficient (η) (eq. 4.1). An anomaly in the results in Tables 5.1 and 5.2 stands out. The 100 cm soil samples with electrets SX6251 and SX6245 were placed inside the

accumulator jar as usual for about 7 days. During the time of the build up inside the jar, a number of hot days were experienced and the specific laboratory was not equipped with an air conditioning unit. Unusual dampness was noticed inside the jar for this measurement, together with the relative higher temperatures might have discharged the electrets more rapidly recording radon concentrations of 877±48 and 854±47 Bq/m^3. These higher radon concentrations correspond to radon emanation coefficients of 0.73±0.04 and 0.71±0.04 respectively. The higher voltage drop was suspected to be from the unusual humid condition inside the jar, and hence would correspond to a higher radon concentration [DeM03]. This was not normal, as can be seen in the results posted in Table 5.1. The experiment was repeated and but none of the results were as extreme as the radon concentrations obtained from that instance.

The soil samples collected at different depths in Table 5.5 show appreciable differences in the emanation coefficient. The samples listed on the left of Table 5.5 are designated ss5cm, ss50cm and ss100cm respectively. This refers to the soil samples from depths at about 5, 50 and 100cm respectively. The 5cm samples recorded a mean of about 0.16, at a depth of about 50cm, a mean of 0.22 was recorded and at 100cm, a value of about 0.36. The increase in the emanation coefficient with depth may suggest that more radon is being released deeper in the dump. This is a surprising result, since the mine dump is assumed to be fairly uniform but may be due to the possible compaction of the soil as the dam dries out over time. The compaction might be caused by dumping the slurry from the processing plant at different times, together with the weight that continually increases with the dumping of more tailings. The data in the rightmost column of Table 5.1 show

Table 5.1 Results obtained using S-Chambers for the emanation studies.

Sample Code	Preference	Electret Serial	Mass (g)	V (Initial)	V (Final)	Time (Days)	Voltage Drop (V)	Calibration Factor	Radon concentration Bq/m^3 ± unc.
M1	Oven-dried	SX6237	34.2	480	378	7.01	102	5.26E-02	245 ± 16
M1	Oven-dried	SX6200	34.2	457	359	7.01	98	5.22E-02	236 ± 15
M2	Oven-dried	SX6256	37.4	460	337	7.01	123	5.21E-02	305 ± 19
M2	Oven-dried	SX6250	37.4	460	340	7.01	120	5.21E-02	297 ± 18
M1 Comp	Oven-dried	SX6243	34.7	512	397	7.00	115	5.30E-02	278 ± 17
M1 Comp	Oven-dried	SX6179	34.7	600	484	7.00	116	5.43E-02	273 ± 17
M1	Room-dried	SX6202	38.4	448	348	6.73	100	5.21E-02	254 ± 16
M1	Room-dried	SX6177	38.4	478	374	6.73	104	5.25E-02	263 ± 17
M2	Room-dried	SX6257	33.0	475	381	6.73	94	5.25E-02	234 ± 15
M2	Room-dried	SX6199	33.0	478	379	6.73	99	5.25E-02	248 ± 16
M1 Comp	Room-dried	SX6310	33.2	526	431	6.73	95	5.33E-02	233 ± 15
M1 Comp	Room-dried	SX6265	33.2	515	419	6.73	96	5.31E-02	237 ± 15
5 cm Soil Sample	Room-dried	SX6237	34.1	570	482	6.88	88	5.41E-02	205 ± 14
50 cm Soil Sample	Room-dried	SX6178	35.4	564	468	6.88	96	5.39E-02	227 ± 15
100 cm Soil Sample	Room-dried	SX6196	32.4	571	439	6.88	132	5.37E-02	325 ± 20
5 cm Soil Sample	20-30% moist	SX6253	33.2	623	361	14.72	262	5.35E-02	300 ± 17
5 cm Soil Sample	20-30% moist	SX6255	33.2	587	311	14.72	276	5.29E-02	323 ± 18
50 cm Soil Sample	20-30% moist	SX6248	43.4	527	132	14.73	395	5.10E-02	494 ± 27
50 cm Soil Sample	20-30% moist	SX6231	43.4	576	201	14.73	375	5.19E-02	458 ± 25
100 cm Soil Sample	20-30% moist	SX6251	41.1	554	236	6.72	318	5.20E-02	877 ± 48
100 cm Soil Sample	20-30% moist	SX6245	41.1	667	347	6.72	320	5.38E-02	854 ± 47
M2 Comp	Room-dried	SX6236	33.4	601	523	6.07	78	5.46E-02	203 ± 14
M2 Comp	Room-dried	SX6263	33.4	463	385	6.07	78	5.25E-02	213 ± 15
M2 Comp	Oven-dried	SX6196	25.4	428	361	6.07	67	5.20E-02	180 ± 13
M2 Comp	Oven-dried	SX6178	25.4	485	417	6.07	68	5.29E-02	180 ± 13
M1	Oven-dried	SX6510	32.2	471	416	6.07	55	5.28E-02	140 ± 11
M1	Oven-dried	SX6252	32.2	444	374	6.07	70	5.22E-02	189 ± 13
5 cm Soil Sample	Room-dried	SX6179	32.3	492	408	7.92	84	5.29E-02	169 ± 11
5 cm Soil Sample	Room-dried	SX6310	32.3	430	346	7.92	84	5.19E-02	172 ± 12
50 cm Soil Sample	Room-dried	SX6254	35.2	480	383	7.92	97	5.26E-02	201 ± 13
50 cm Soil Sample	Room-dried	SX6265	35.2	409	306	7.92	103	5.14E-02	221 ± 14
100 cm Soil Sample	Room-dried	SX6184	31.8	655	480	7.92	175	5.47E-02	372 ± 22
100 cm Soil Sample	Room-dried	SX6260	31.8	691	526	7.92	165	5.53E-02	344 ± 20

Table 5.2 Radon emanation coefficients calculated from S-Chamber results.

Sample Code	Preference	Electret Serial	Mass (g)	Volume (l)	K	RnERaC Bq/kg ± unc.	A_{Ra} Content (Bq/kg) ± unc.	Rn Emanation Coefficient ± unc.
M1	Oven-dried	SX6237	34.2	3.72	2.305	61 ± 4	233 ± 6	0.26 ± 0.02
M1	Oven-dried	SX6200	34.2	3.72	2.305	59 ± 4	233 ± 6	0.25 ± 0.02
M2	Oven-dried	SX6256	37.4	3.72	2.305	70 ± 4	252 ± 7	0.28 ± 0.02
M2	Oven-dried	SX6250	37.4	3.72	2.305	68 ± 4	252 ± 7	0.27 ± 0.02
M1 Comp	Oven-dried	SX6243	34.7	3.72	2.306	69 ± 4	256 ± 8	0.27 ± 0.02
M1 Comp	Oven-dried	SX6179	34.7	3.72	2.306	67 ± 4	256 ± 8	0.26 ± 0.02
M1	Room-dried	SX6202	38.4	3.72	2.369	58 ± 4	233 ± 6	0.25 ± 0.02
M1	Room-dried	SX6177	38.4	3.72	2.369	60 ± 4	233 ± 6	0.26 ± 0.02
M2	Room-dried	SX6257	33.0	3.72	2.368	62 ± 4	252 ± 7	0.25 ± 0.02
M2	Room-dried	SX6199	33.0	3.72	2.368	66 ± 4	252 ± 7	0.26 ± 0.02
M1 Comp	Room-dried	SX6310	33.2	3.72	2.368	62 ± 4	256 ± 8	0.24 ± 0.02
M1 Comp	Room-dried	SX6265	33.2	3.72	2.368	63 ± 4	256 ± 8	0.25 ± 0.02
5 cm Soil Sample	Room-dried	SX6237	34.1	3.84	2.334	54 ± 4	313 ± 9	0.17 ± 0.01
50 cm Soil Sample	Room-dried	SX6178	35.4	3.84	2.333	57 ± 4	251 ± 6	0.23 ± 0.02
100 cm Soil Sample	Room-dried	SX6196	32.4	3.84	2.334	90 ± 5	259 ± 6	0.35 ± 0.02
5 cm Soil Sample	20% Wet	SX6253	33.2	3.72	1.535	52 ± 3	313 ± 9	0.17 ± 0.01
5 cm Soil Sample	20% Wet	SX6255	33.2	3.72	1.535	55 ± 3	313 ± 9	0.18 ± 0.01
50 cm Soil Sample	20% Wet	SX6248	43.4	3.72	1.535	65 ± 3	251 ± 6	0.26 ± 0.02
50 cm Soil Sample	20% Wet	SX6231	43.4	3.72	1.535	60 ± 3	251 ± 6	0.24 ± 0.01
100 cm Soil Sample	20% Wet	SX6251	41.1	3.72	2.370	188 ± 10	259 ± 6	0.73 ± 0.04
100 cm Soil Sample	20% Wet	SX6245	41.1	3.72	2.370	183 ± 10	259 ± 6	0.71 ± 0.04
M2 Comp	Room-dried	SX6236	33.4	3.72	2.540	57 ± 4	286 ± 8	0.20 ± 0.01
M2 Comp	Room-dried	SX6263	33.4	3.72	2.540	60 ± 4	286 ± 8	0.21 ± 0.02
M2 Comp	Oven-dried	SX6196	25.4	3.72	2.540	67 ± 5	286 ± 8	0.23 ± 0.02
M2 Comp	Oven-dried	SX6178	25.4	3.72	2.540	67 ± 5	286 ± 8	0.23 ± 0.02
M1	Oven-dried	SX6510	32.2	3.72	2.540	41 ± 3	233 ± 6	0.18 ± 0.01
M1	Oven-dried	SX6252	32.2	3.72	2.540	55 ± 4	233 ± 6	0.24 ± 0.02
5 cm Soil Sample	Room-dried	SX6179	32.3	3.72	2.132	41 ± 3	313 ± 9	0.13 ± 0.01
5 cm Soil Sample	Room-dried	SX6310	32.3	3.72	2.132	42 ± 3	313 ± 9	0.14 ± 0.01
50 cm Soil Sample	Room-dried	SX6254	35.2	3.72	2.131	45 ± 3	251 ± 6	0.18 ± 0.01
50 cm Soil Sample	Room-dried	SX6265	35.2	3.72	2.131	50 ± 3	251 ± 6	0.20 ± 0.01
100 cm Soil Sample	Room-dried	SX6184	31.8	3.72	2.131	93 ± 5	259 ± 6	0.36 ± 0.02
100 cm Soil Sample	Room-dried	SX6260	31.8	3.72	2.131	86 ± 5	259 ± 6	0.33 ± 0.02

Table 5.3 Results obtained using S-Chambers for the emanation studies.

Sample Code	Preference	Electret Serial	Mass (g)	V (Initial)	V (Final)	Time (Days)	Voltage Drop (V)	Calibration Factor	Radon concentration $Bq/m^3 \pm$ unc.
5 cm Soil Sample	Room-dried	SX6182	38.8	484	414	20.85	70	8.74E-03	340 ± 24
5 cm Soil Sample	Room-dried	SX6234	38.8	465	396	20.85	69	8.67E-03	337 ± 24
50 cm Soil Sample	Room-dried	SX6254	37.2	562	483	20.86	79	9.02E-03	376 ± 26
50 cm Soil Sample	Room-dried	SX6261	37.2	538	458	20.86	80	8.93E-03	385 ± 26
100 cm Soil Sample	Room-dried	SX6233	37.5	568	442	20.86	126	8.95E-03	630 ± 39
100 cm Soil Sample	Room-dried	SX6244	37.5	568	441	20.86	127	8.95E-03	636 ± 39
5 cm Soil Sample	Room-dried	SX6235	32.9	272	185	27.72	87	7.92E-03	352 ± 23
5 cm Soil Sample	Room-dried	SX6232	32.9	282	198	27.72	84	7.96E-03	336 ± 23
50 cm Soil Sample	Room-dried	SX6253	43.1	336	227	27.73	109	8.12E-03	440 ± 28
50 cm Soil Sample	Room-dried	SX6251	43.1	216	110	27.73	106	7.67E-03	454 ± 29
100 cm Soil Sample	Room-dried	SX6204	40.9	365	163	27.72	202	8.05E-03	861 ± 49
100 cm Soil Sample	Room-dried	SX6205	40.9	369	172	27.72	197	8.07E-03	836 ± 48

Table 5.4 Radon emanation coefficients calculated from L-Chamber results.

Sample Code	Preference	Electret Serial	Mass (g)	Volume (l)	K	RnERaC Bq/kg ± unc.	A_{Ra} Content (Bq/kg) ± unc.	Rn Emanation Coefficient ± unc.
5 cm Soil Sample	Room-dried	SX6182	38.8	3.87	1.349	46 ± 3	313 ± 9	0.15 ± 0.01
5 cm Soil Sample	Room-dried	SX6234	38.8	3.87	1.349	45 ± 3	313 ± 9	0.14 ± 0.01
50 cm Soil Sample	Room-dried	SX6254	37.2	3.87	1.349	53 ± 4	251 ± 6	0.21 ± 0.02
50 cm Soil Sample	Room-dried	SX6261	37.2	3.87	1.349	54 ± 4	251 ± 6	0.22 ± 0.02
100 cm Soil Sample	Room-dried	SX6233	37.5	3.87	1.348	88 ± 5	259 ± 6	0.34 ± 0.02
100 cm Soil Sample	Room-dried	SX6244	37.5	3.87	1.348	89 ± 5	259 ± 6	0.34 ± 0.02
5 cm Soil Sample	Room-dried	SX6235	32.9	3.87	1.246	52 ± 3	313 ± 9	0.16 ± 0.01
5 cm Soil Sample	Room-dried	SX6232	32.9	3.87	1.246	49 ± 3	313 ± 9	0.16 ± 0.01
50 cm Soil Sample	Room-dried	SX6253	43.1	3.87	1.246	49 ± 3	251 ± 6	0.20 ± 0.01
50 cm Soil Sample	Room-dried	SX6251	43.1	3.87	1.246	51 ± 3	251 ± 6	0.20 ± 0.01
100 cm Soil Sample	Room-dried	SX6204	40.9	3.87	1.246	102 ± 6	259 ± 6	0.39 ± 0.02
100 cm Soil Sample	Room-dried	SX6205	40.9	3.87	1.246	99 ± 6	259 ± 6	0.38 ± 0.02

Table 5.5 Summary of results from radon emanation studies using E-PERM technology.

From Emanation Depth Sampling point					M1 and M2 Locations				
Site Location	Preference	SST/LST	Emanation Coefficient	Eman. Coeff. SD	Site Location	Preference	SST/LST	Emanation Coefficient	Eman. Coeff. SD
SS5cm	Room-dried	SST	0.17	0.01	M1	Oven-dried	SST	0.23	0.03
SS5cm	20-30% moist	SST	0.17	0.02	M1C	Oven-dried	SST	0.27	0.03
SS5cm	Room-dried	SST	0.13	0.01	M1	Room-dried	SST	0.25	0.02
SS5cm	Room-dried	LST	0.15	0.02	M1C	Room-dried	SST	0.24	0.02
SS5cm	Room-dried	LST	0.16	0.02					
					M2	Oven-dried	SST	0.27	0.03
SS50cm	Room-dried	SST	0.23	0.02	M2C	Oven-dried	SST	0.23	0.03
SS50cm	20-30% moist	SST	0.25	0.02	M2	Room-dried	SST	0.26	0.02
SS50cm	Room-dried	SST	0.19	0.02	M2C	Room-dried	SST	0.21	0.02
SS50cm	Room-dried	LST	0.21	0.02					
SS50cm	Room-dried	LST	0.20	0.02					
SS100cm	Room-dried	SST	0.35	0.02					
SS100cm	Room-dried	SST	0.34	0.03					
SS100cm	Room-dried	LST	0.34	0.03					
SS100cm	Room-dried	LST	0.39	0.03					

consistent results within 1 standard deviation throughout for the soil-gas measurements at the two sites designated M1 and M2, for the samples collected close to the surface. It also shows that the results compare well independently of the preparation method. A follow up study is suggested to measure the radon emanation coefficient at the different depths considered for soil-gas measurements to investigate how the radon emanation coefficient correlates to the radon soil-gas concentration in the pore space. SST and LST refer to the specific EIC's that were used together with the electret type. SST refers to an S-chamber together with a ST-electret (short-term) and LST refers to an L-chamber used with a ST-electret. The S-chamber was used for short-term (≈7days) measurements whereas the L-chamber was used for long-term (≈1month) measurements. The sample codes M1, M1C, M2 and M2C refer to the samples Medusa 1, Medusa 1 composite, Medusa 2 and Medusa 2 composite respectively. The composite part refers to an array of samples that was collected at a distance of 1 m away from M1 or M2. It was processed through sieving and by removing all stones and debris present in the soil. It was then mixed thoroughly to form the composite samples.

Throughout the radon emanation experiments, the room temperature was recorded at about 25°C, which is about the same for environmental measurements. In these conditions, the E-PERMs show very good stability in their readings. The radium content was found to be reasonably constant with depth, but a definite increase in the radon emanation can be observed as is evident in table 5.5. The 5cm samples show an emanation coefficient percentage of about 16%, the 50cm samples of 22% and the 100cm samples of 36%. The increased emanation is a surprising result since at first the whole dump was considered uniform in the texture of the soil. A possible reason might be that more radium might be concentrated on the surface of the grain

particles, leading to an increased radon emanation, relative to that measured from samples closer to the surface. The radium content of the soil was then also determined at iThemba LABS by sealing the samples in Marinelli beakers so that the radium reaches secular equilibrium with its decay products, while the radon emanation power was determined at UWC.

5.3 Radium Content

Section 4.5 describes the preparation of the soil samples for counting, using an HPGe gamma-ray detector. The results are listed in Table 5.6. The main interest in Table 5.6 is the uranium content from the radiometric study. The uranium content was measured using lines from the radon decay products. The thorium and potassium contents show a relative level of consistency in the radiometric properties of the mine dump soil. The observed values for the ^{40}K activity concentrations are quite normal, whereas the thorium content is very low throughout the range of depth samples as well as those collected near the surface. The radium content was used for two purposes. The first is to calculate the radon emanation fraction as in chapter 4. The second

Table 5.6 Results of the radiometric sample analysis.

Sample Code	Depth in Mine Dump	Uranium Content	Thorium Content	Potassium Content
M1	Surface	233 ± 6	17 ± 4	208 ± 6
M1C	Surface	256 ± 8	19 ± 2	226 ± 7
M2	Surface	252 ± 7	15 ± 2	215 ± 6
M2C	Surface	286 ± 8	22 ± 2	244 ± 7
SS5cm	≈5cm	313± 9	21 ± 8	228 ± 7
SS50cm	≈50cm	251 ± 6	13 ± 5	211 ± 6
SS100cm	≈100cm	259 ± 7	15 ± 5	174 ± 6

use of the radium content is for calculating the maximum predicted radon concentration in the mine dump soil using the relation in chapter 3, eq. (3.16) for reference purposes, but it can also be used to calculate the production rate of radon (the term S in eq. 3.16) in the pore space. The radium content is also suspected to be a little bit lower than measured, since radon can escape via emanation in the preparation before measuring the radium content as well as through the processing of the sample. Secular equilibrium is assumed when determining the ^{226}Ra content. It should also be noted that the uncertainties quoted are statistical errors.

5.4 Radon Soil-gas Experiments on the Gold Mine Dump

Measurements of the radon soil-gas were taken at Kloof mine dump. Table 5.7 and Fig. 5.1 show the results obtained from the measurements. The measurement at location M1 shows a much more rapid increase with depth in the radon soil-gas. It would suggest that the radon concentration would increase to its maximum much faster than that at the point M2. Considering the plot in Fig. 5.2 with varied radon concentrations from the modelling part of

Table 5.7 RAD7™ Results from M1 and M2 on Kloof Mine Dump. The uncertainties were purely due to counting statistics as indicated by the RAD7.

M1			M2		
Depth (cm)	Mean Rn Conc. (kBq/m^3)	Std Dev (kBq/m^3)	Depth (cm)	Mean Rn Conc. (kBq/m^3)	Std Dev (kBq/m^3)
25	8.1	0.8	25	11.6	0.5
50	129.1	4.2	50	49.7	1.3
75	277.6	5.7	75	163.1	2.9
100	350.0	6.3	100	226.5	7.1
120	405.8	13.8	120	271.4	13.9

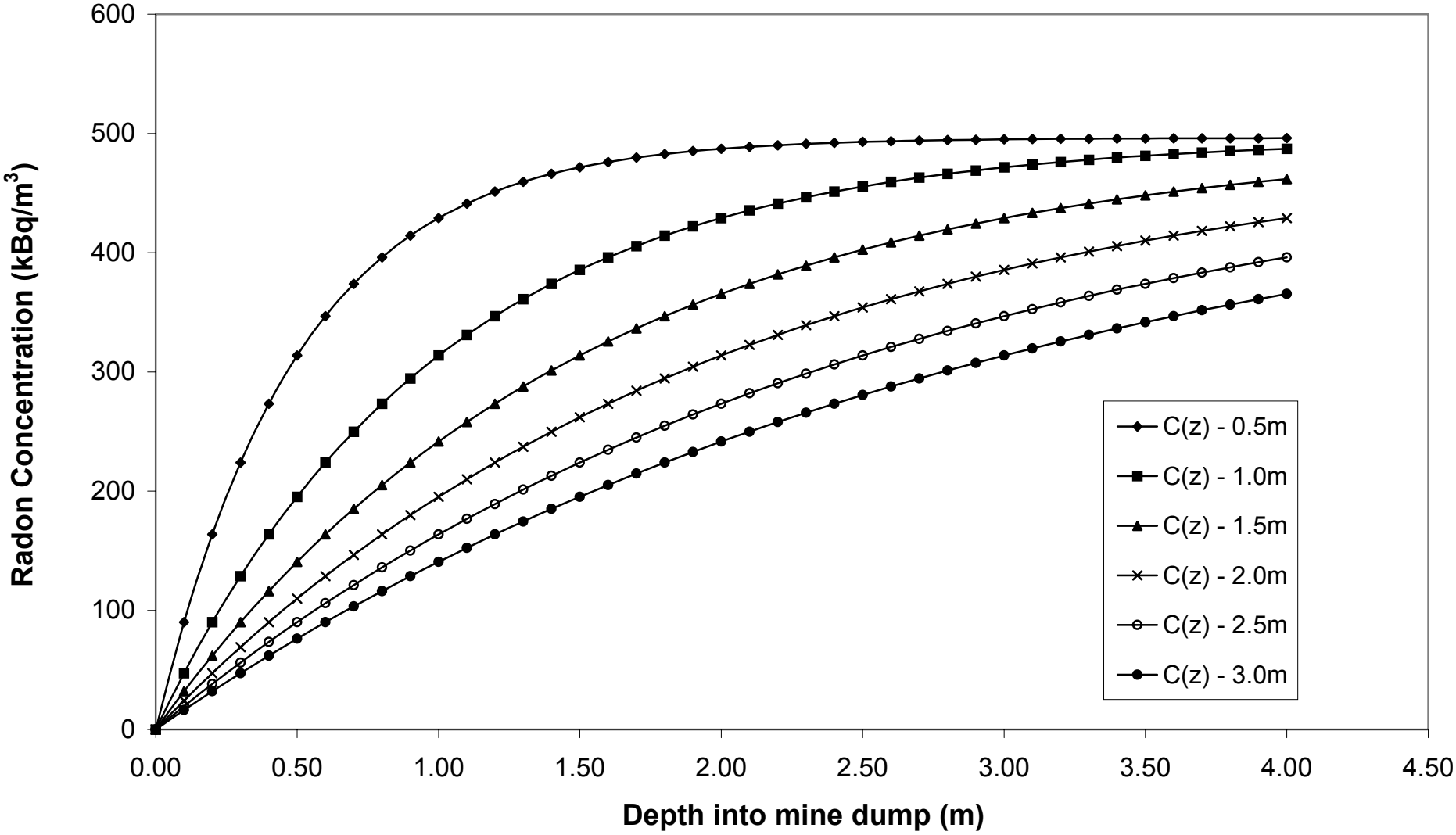

Figure 5.2 One-dimensional radon soil-gas modelling on a mine dump. The lengths indicated in the legend are the diffusion lengths.

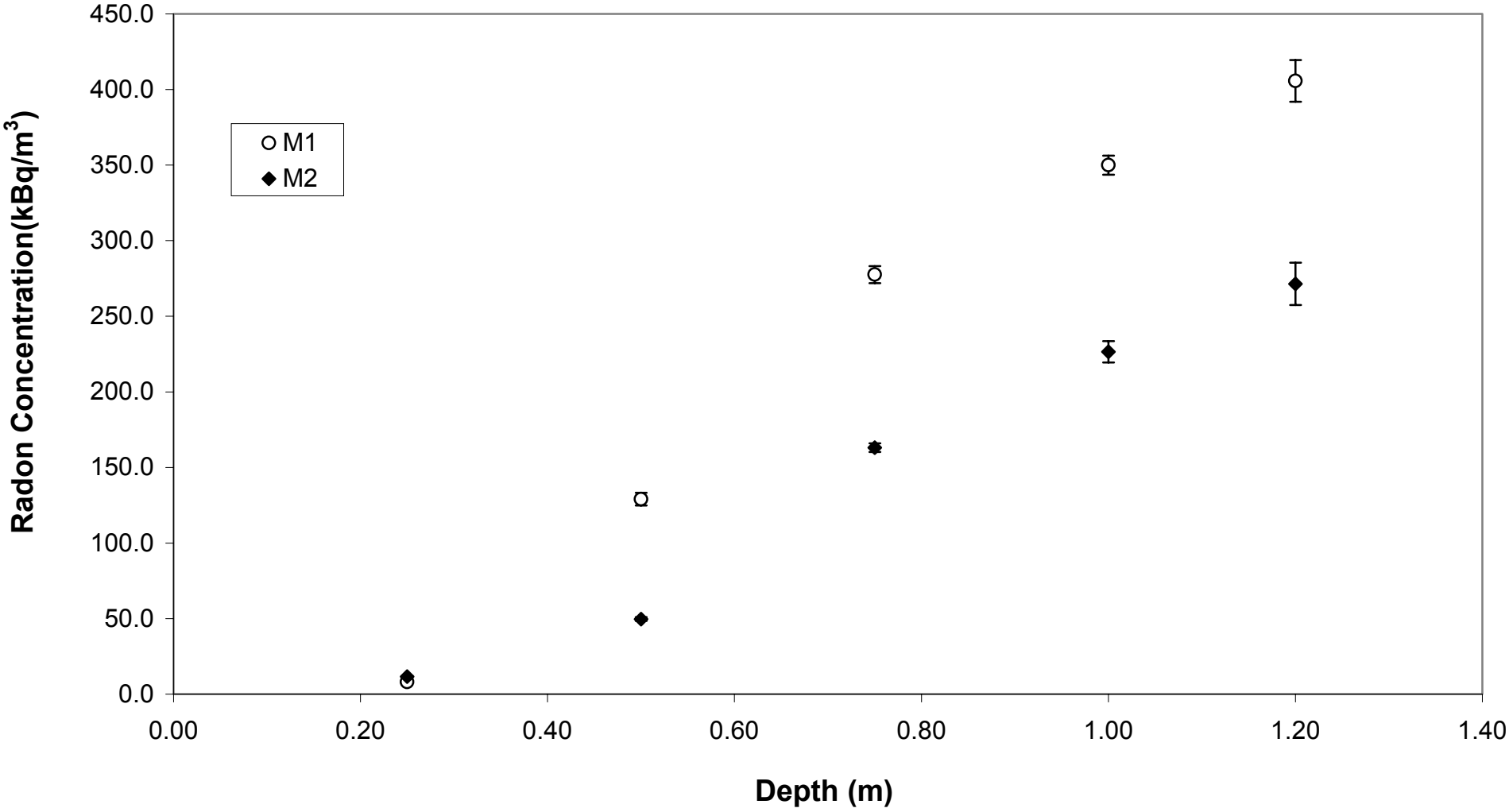

Figure 5.1 RAD7™ results of November 2002 experiments on the mine dump at points M1 and 2.

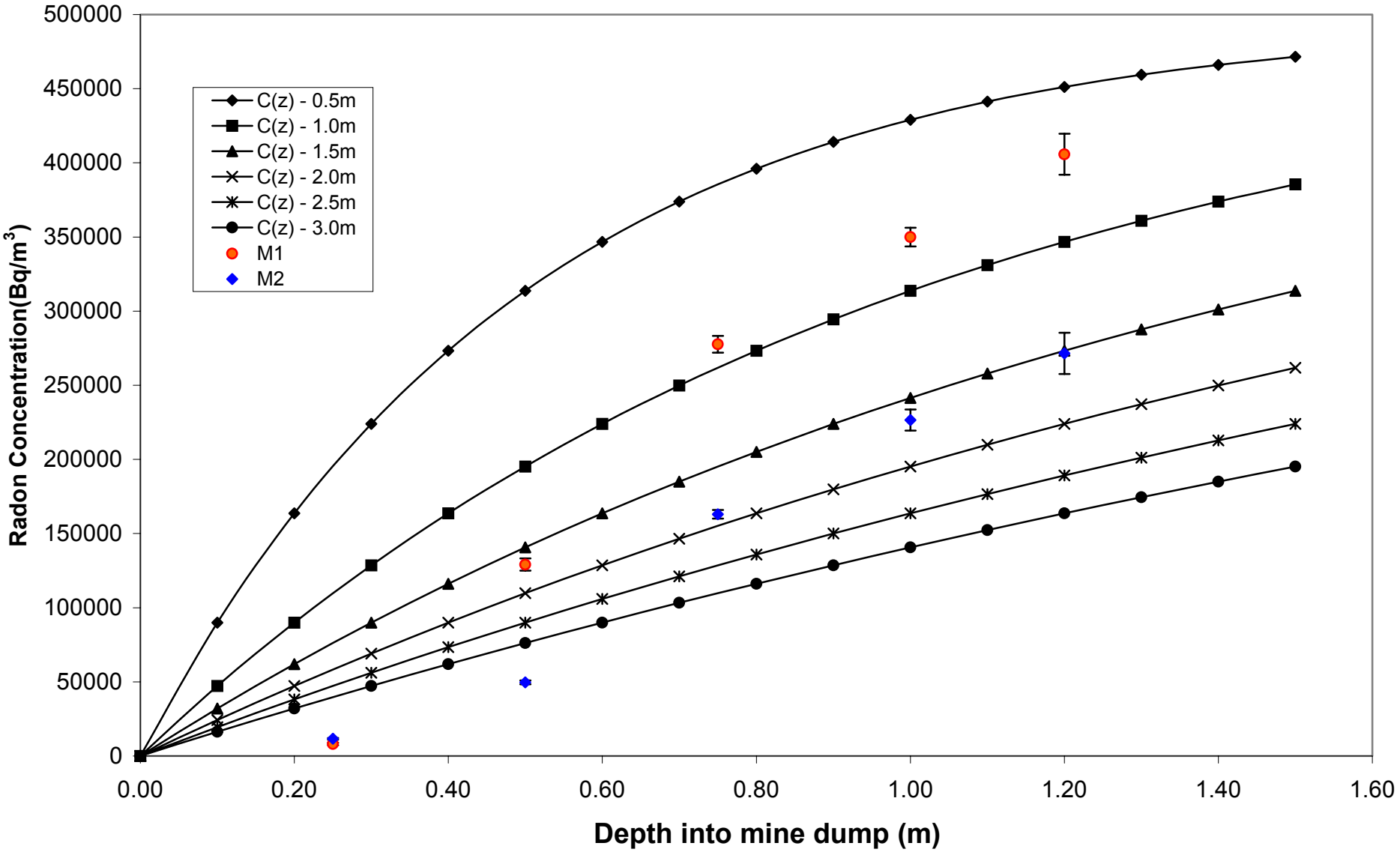

Figure 5.3 Plots of the modelling of the radon soil-gas concentration with that of the actual RAD7 results. The lengths indicated in the legend are the diffusion lengths.

the experiment, it would be safe to conclude that the diffusion length at that point of the mine dump for radon is less than that at M2 and since the diffusion length and the radon diffusion coefficient (D) are linked (eq. 3.19), it follows that the radon soil gas at point M1 diffuses much slower than at M2, which is interesting, since the soil in the dump is considered uniform. The 2 points were chosen based on a survey of the mine dump using the MEDUSA in-situ γ-ray detector. The point M1 showed a lower uranium activity concentration than point M2.

The actual depth profile in Fig. 5.1 is compared to the predicted depth profile in Fig. 5.2 by overlaying the results as in Fig. 5.3. The values obtained at the shallower depths appear to be too low, as mentioned before. A possible reason could be that the pressure on the surface influences the measurements at these lower depths or, more likely, the measurements at small depths suffer from a leakage of air down the side of the probe when taking measurements. The possible difference in compaction of the soil could also explain the more rapid increase in the soil-gas concentration at different sites. This would mean that less radon would diffuse to the surface as more and more radon is potentially trapped in the interstitial pore space of the soil. In the analytical model, the soil is assumed uniform throughout the dump and any soil compaction is not included.

Measurements up to 1.25 meters were possible because of the length of the probe. At shallower depths, the radon concentration is very low if compared to the modelled values that will be discussed later in this section. reduce the radon soil-gas concentration. Another reason that might influence the radon concentrations at depths of about 20-50 cm in the dump is the air pressure at the surface of the dump. Variations in the air pressure in the soil have been

studied by van der Spoel et al. under specific conditions in the laboratory [Spo98b]. Measurements on a mine dump at greater depths will be useful in discriminating between different models. The mine dump soil, as already mentioned, consists of finer-grained particles, almost similar to clay, but not as compact. The optimum suggested depth to consider radon soil-gas measurements is about 1m, unless the soil consists of coarser grained particles, in which case, deeper measurements are acceptable [Åke97]. This depth also minimises the risk of meteorological changes affecting the soil-gas concentrations and the soil air is considered relatively constant. These changes include air pressure, air humidity, air temperatures and wind speeds.

The diffusion equation listed in chapter 3, section 3.7 has been solved to obtain eq. (3.19). Figure 5.2 represents the radon concentration depth profile calculated from eq. (3.19) for different l values. A maximum depth (z) of 4m was chosen to show how the concentration increases exponentially to reach a maximum concentration irrelevant of time. The results from which Fig. 5.1 was plotted, are grouped in a table in Appendix C. These predictions assume that only diffusion is considered to have an effect on the radon soil-gas. It is clear from the graph that a very short diffusion length (l) would cause a very rapid increase in the radon soil-gas with increasing depth as indicated by the curve C(z) – 0.5m.

The analytical model does not clearly explain the radon concentrations at shallower depths. The model predicts radon concentrations that tend to a maximum concentration of about 490 kBq/m^3. This is calculated using equation (3.16). The input parameters that were used to calculate C_{Max} are the radon emanation coefficient, η, the specific bulk density, ρ_s, the radium content, A_{Ra} and the soil porosity, ε. The model assumes a constant A_{Ra},

whereas the measurements of the samples brought back from the mine dump indicate that this is not quite true throughout. Equation (3.17) is used for the determination of the creation rate of radon, S, is also assumed constant and not changing that in turn is used to calculate C_{max}. See Appendix C, for calculation of C_{max}.

5.5 Determination of the Mine Dump Soil Porosity, Specific and Bulk Densities

The soil porosity of the samples collected was analysed in the laboratory at UWC. The results are presented in Table 5.8 and were determined by using the method described in chapter 4, section 4.6. The compaction of the soil throughout the experiment was observed not to be as compact as when undisturbed. The compaction however is a result of the continuous filling of the dump with the slurry. However, our method includes the soil samples being immersed in a known amount of water and left to stand for about 1-2 hours for the soil to settle after all the air is being shaken from the volumetric

Table 5.8 Results of the total soil porosity of the mine dump soil.

Soil Type	Mass of Soil (g)	Volume of Soil (cm^3)	Volume of Water (cm^3)	Volume of Soil & Water	Porosity (vol.) of Soil (cm^3)	Porosity of Soil
Mine Dump	50.4	34	52	73	13	0.38 ± 0.09
"	49.9	33	50	72	11	0.33 ± 0.09
"	50.9	35	51	74	12	0.34 ± 0.09
"	50.6	34	51	73	12	0.35 ± 0.09
"	51.1	32	49	70	11	0.34 ± 0.09
					AM $\pm$ SD	0.35 ± 0.02

flask. This would make sure that the porosity measured would be close to the initial porosity of the soil. The arithmetic mean obtained from the results for the total porosity is 0.35 ± 0.02. The specific density ρ_s was determined using the method described in chapter 4, section 4.7. The bulk density ρ_b of the soil is directly related to the specific density and porosity and can be calculated by using eq. (4.13). The results are presented in Table 5.9. The experiment was repeated several times and the arithmetic mean was recorded to be 2846 ± 287 kg/m^3. The calculation of the bulk density followed with an average value of 1850 ± 186 kg/m^3.

Table 5.9 Results of the specific and bulk densities of the mine dump soil.

Soil Type	M_w (g)	M_s (g)	V_f (ml)	ρ_s (kg/m^3)	ρ_b (kg/m^3)
Mine Dump	495.7	31.7	510	2403 ± 48	1562 ± 94
"	488.4	32.2	500	3064 ± 62	1992 ± 121
"	486.8	35.3	500	2914 ± 59	1894 ± 115
"	485.5	41.7	500	3108 ± 63	2021 ± 122
"	487.3	31.8	500	2739 ± 55	1780 ± 108
			AM ± SD	2846 ± 287	1850 ± 186

The specific density of the soil is believed to be quite high relatively to a plain sand sample, but this can be expected, as the mine dump soil is finely grounded and treated with chemicals to extract the gold and traces of uranium would be evident in this enhanced state. It might also be the case that the mine dump material are quite different from silicon oxide [Gra05].

5.6 Summary

In this chapter, the main results have been presented. The parameters obtained conclude that which is needed to complete the numerical modelling of the radon diffusion equation. The radon emanation coefficient results clearly show an increase with increasing depth into the mine dump. The usage of different Electret Ion Chamber configurations showed that the emanation could be measured independently of what chamber is used, considering that the right exposure times are used. The samples from the surface points M1 and 2, shows good agreement in the radon emanation, even though composite samples were generated for completeness. The results from the radiometric studies show a fair agreement, the uranium content, as well as in the thorium and potassium activity concentrations.

The radon emanation coefficient, specific and bulk densities of the soil, the porosity and the radium content was determined to complete the calculation of the maximum radon concentration (eq. 3.16) for that specific dump to validate the model through in-situ experiments. The in-situ experiments involved measurements with the RAD7 electronic radon detector, to compare the results to that generated from the modelling. The data obtained from these measurements are plotted in Fig. 5.3 together with the modelled data, and it can be noted that the M1 measurement increases clearly much faster than that at point M2. Now, in Fig. 5.3, only the curves for the diffusion lengths of increments of 50 cm are plotted, but those in between can be generated to investigate the correlation between modelled and measured data. Another point to note in Fig 5.3 for the measurements M1 and 2, is that the first 2 points in the profile can be neglected, since the measured data might not clearly reflect the actual value, because of problems with a

sufficient seal around the probe in the soil at these shallow depths as well as meteorological effects. The bottom line is that there is still work to be done to predict the actual radon concentration, given the right dimensions and factors are more clearly investigated. The model therefore consists of three parts: the first part includes solving the radon diffusion equation. The second part of the process is to determine the parameters that would uniquely identify the source (emanation coefficient, porosity, etc.) and thirdly, to validate the data from the in-situ measurements using the relevant model.

Chapter 6

Conclusion

This study included a one-dimensional steady-state model that was derived in predicting the radon concentration inside a dump and can be refined to more realistically predict the soil-gas concentration by considering the effects of pressure on the dump itself as well as the time dependence. This will of course lead to other complexities to be considered. One of the factors will be that the radon diffusion equation must be expressed in terms of 3 dimensions, and not as a function of depth as in the case of this model. The model itself is also just one of the key parameters that needs to be assessed, together with the radon flux of the source to assess the possible risk to critical groups surrounding the source. These sources may include tailings dams, phosphate rock plants and unregulated dumping sites from the mining processes or neglect due to a specific site being ownerless. The results from this study, therefore, play an important role in the understanding and predicting the radon flux from a typical mine dump.

The radon flux (exhalation) from a mine dump is dictated by 2 processes. The first has to do with the radon emanation constant, which can be determined from soil samples collected at the source. The soil samples were tested for radon emanating from ^{226}Ra bearing soil (RnERaC) as well as the radium content, A_{RA}, to eventually record the radon emanation factor. The results range overall from about 0.13 till about 0.39. The results were however grouped according to depth into the dump. The 5cm soil samples recorded an average of 0.16 ± 0.04, the 50cm samples 0.22 ± 0.05 and lastly the 100cm samples 0.36 ± 0.06. The surface samples at the points M1 and 2 recorded

averages of 0.25±0.05 and 0.24±0.05 respectively. The radiometric analysis of the samples collected showed a reasonable amount of agreement. The uranium ranged from about 233±6 Bq/kg till 313±9Bq/kg. The second process includes the radon transport through the medium. The migration can be dictated by diffusion or advection or by both in some cases. There are also a few factors that are needed for those processes; which include the porosity, specific and bulk densities, and in some cases, the moisture content and grain-size distributions of the soil considered. The average porosity were calculated at 0.35±0.02. The average specific and bulk densities were recorded as 2846±287 kg/m^3 and 1850±186 kg/m^3 respectively. The radon would be potentially trapped inside the body of the mine dump, but could be released through meteorological processes or the most common, diffusion.

The radon soil-gas measurements taken throughout this study show extremely high readings, but a marginal fraction only reach the surface of the dump as was assessed by Lindsay et al. [Lin04]. The depth profiling might also be a useful tool in deriving the radon diffusion length. The practicality of the RAD7 detector was proved here for the purpose of making in-situ measurements that are readily available and free for interpretation. On a more quantative basis, those results can then be correlated with the predicted ones. The results for the radon soil-gas measurements range from 8.1±0.8 kBq/m^3 till round about 405.8±13.8 kBq/m^3. The uncertainties showed as standard deviations since the measurement is a composite of 4 measurements per cycle. The low uncertainties are purely due to counting statistics as measured by the RAD7. The point M2 showed values from about 11.6±0.5 kBq/m^3 till round about 271.4±13.9 kBq/m^3.

The methods used to investigate the emanation capability of the mine dump soil, proved to be quite consistent, depending on your exposure periods and the type of detector that will be used. These factors will then play a role in the radiological assessment of mine dumps, in preparation for radiation protection, restoration or rehabilitation activities for the site. Mine dumps cover a great deal of area (in the Gauteng province especially), and since all land with radioactive residue need to be assessed and reviewed by the regulatory authority, a good, fast and efficient strategy is needed to deal with the issues. These field and laboratory measurements would then be just the first step in the assessment process, next would be the identification of the possible and relevant pathways from the source term, and finally followed by the risk estimation.

References

[Åke97] Åkerblom, G., Mellander, H. (1997) Geology and radon. In Radon measurements by etched track detectors, Editors S.A. Durrani and R. Ilić, World Scientific Publishing Co. Pty. Ltd.

[Ald94] Aldenkamp, F.J. (1994) In situ radon exhalation meter, In Doctorate thesis of F.J. Aldenkamp and P. Stoop, Groningen: Rijksuniversiteit Groningen.

[Big84] Bigu, J. (1984) Study of radon concentration, surface radon flux and other radiation variables from uranium mine tailings areas. Uranium 1, pp 257 - 277.

[Bos03] Bossew, P. (2003) The radon emanation power of building materials, soils and rocks. Applied Radiation and Isotopes, Vol. 59, pp389 – 392.

[Bra03] Braga, I. (2003) Treatment of environmental liability in urban areas – MMV experience. Proceedings of Mining and Sustainable Development Conference, Sandton, South Africa, Vol. 1, 3C – 1.

[Cam02] Cambridge Physics: Discovery of the nucleus (2002) (Online). Available at http://phy.cam.ac.uk/camphy/nucleus/nucleus2_1.htm Last updated 4 February.

[Cha03] Chamber of Mines of South Africa (2003) Mining and sustainable development conference, Conference Handbook, pp 15.

[Col95] Collé, R., Kotrappa, P., Hutchinson, J.M.R. (1995) Calibration of electret-based integral radon monitors using NIST polyethylene-encapsulated $^{226}Ra/^{222}Rn$ emanation (PERE) standards. Journal of Research of the National Institute of Standards and Technology, Vol. 100, pp 629 – 639.

[Con99] Conway, T. (1999). Two methods of investigating the effects of soil particle size on soil porosity. Sci-Journal, Vol. 4, no.2. (Online) http://www.sci-journal.org/index.php?link=report.php

[Cra75] Crank, J. (1975) The mathematics of diffusion, Oxford: Clarendon Press.

[DeM01] de Meijer, R.J., Lindsay, R., Maleka, P., Newman, R.T. (2001) Proposal to assess the integral radon production of gold-mine dumps. Internal report, iThemba LABS.

[DeM03] de Meijer, R.J., (2003) Private communication.

[Dur00] Durridge Company Inc. (2000), Reference Manual version 6.0.1, RAD7™ Electronic Radon Detector.

[EPA92] U.S. Environmental Protection Agency, Office of Air and Radiation (6604J) (1992), Indoor radon and radon decay product measurement device protocols (Online) http://www.epa.gov/radon/pubs/devprot1.html. Last updated 24 March 2003.

[Fle97] Fleischer, R.L. (1997) Radon: Overview of properties, origin and transport. In Radon measurements by etched track detectors, Editors S.A. Durrani and R. Ilić, World Scientific Publishing Co. Pty. Ltd.

[Gad95] Gadd, M.S., Borak, T.B. (1995) In-situ determination of the diffusion coefficient of ^{222}Rn in concrete. Health Physics, Vol. 68, no. 6, pp 817 – 822.

[Geo84] George, A.C. (1984) Passive integrated measurements of indoor radon using activated carbon. Health Physics, Vol.46, no. 4, pp 867 – 872.

[Ger04] Gervino, G., Bonetti, R., Cigolini, C., Marino, C., Prati, P., Pruiti, L. (2004). Environmental radon monitoring: comparing drawbacks and performances of charcoal canisters, alpha-track and E-PERM detectors. Nuclear Instruments and Methods in Physics Research A, Vol. 518, pp 452 – 455.

[God02] Godoy, M., Hadler, J.C., et al. (2002) Effects of environmental conditions on the radon daughters spatial distribution. Radiation Measurements, Vol. 35, pp 213 – 221.

[Gra05] van der Graaf, E. (2005) Private communication.

[Hay03] Hayes, R., Cheng Chiou, H. (2003) Preliminary evaluation of real time false CAM alarm through continuous radon monitoring. Health Physics, Vol. 84, no. 5, pp 589 – 592.

[Jam88] James, A.C. (1988) Lung dosimetry. Radon and its decay products in indoor air. Editors W. Nazaroff and A. Nero, John Wiley and Sons, Inc. pp 266.

[Kot00] Kotrappa, P. (2000) Performance of E-PERM electret ion chamber radon monitors at very high temperatures and in the presence of microbial activity. Health Physics, Vol. 78, no. 2, pp 228.

[Kot88] Kotrappa, P., Dempsey, J., Hickey, J.R., Stieff, L.R. (1988) An electret passive environmental ^{222}Rn monitor based on ionization measurements. Health Physics, Vol. 54, pp 47 – 56.

[Kot90] Kotrappa, P., Dempsey, J.C., Ramsey, R.W., Stieff, L.R. (1990) A practical E-PERM (Electret Passive Environmental Radon Monitor) system for indoor ^{222}Rn measurement. Health Physics, Vol. 58, no. 4, pp 461 – 467.

[Kot92a] Kotrappa, P., Brubaker, J., Dempsey, J.C., Stieff, L.R. (1992) Electret ion chamber system for measurement of environmental radon and environmental gamma radiation. Radiation Protection Dosimetry, Vol. 45, no.1-4, pp 107 – 110.

[Kot92b] Kotrappa, P., Stieff, L.R. (1992) Elevation correction factors for E-PERM radon monitors. Health Physics, Vol. 62, no. 1, pp 82 - 86.

[Kot94] Kotrappa, P., Stieff, L.R. (1994) Application of NIST ^{222}Rn emanation standards for calibrating ^{222}Rn monitors. Radiation Protection Dosimetry, Vol. 55, no. 3, pp 211 – 218.

[Kra88] Krane, K.S. (1988) Alpha Decay. Introductory Nuclear Physics. John Wiley and Sons, Inc., New York, pp 246 – 271.

[Kum03] Kumar, R., Sengupta, D., Prasad, R. (2003). Natural radioactivity and radon exhalation studies of rock samples from Surda Copper deposits in Singhbhum shear zone. Radiation Measurements, Vol. 36, pp 551 – 553.

[Lin04] Lindsay, R., de Meijer, R.J., Newman, R.T., Motlhabane, T.G.K., Maleka, P. (2004) Monitoring the radon flux from gold-mine dumps by gamma ray mapping. Nuclear Instruments and Methods in Physics Research, B213, pp 775 – 778.

[Liv90] Livingston, J.V., Jester, W.A. (1990) Measurement of radon flux from undisturbed soil using E-PERM detectors. Master's thesis of J.V. Livingston, The Pennsylvania State University.

[Mar92] Markkanen, M., Arvela, H. (1992) Radon emanation from soils. Radiation Protection Dosimetry, Vol. 45, no. 1, pp 269 – 272.

[Mot03] Motlhabane, T.G.K., Tsela, A., Lindsay, R., de Meijer, R.J., Newman, R.T., Speelman, W.J., Joseph, A.D., Maphoto, K. (2003) Monitoring the radon flux from gold-mine dumps by gamma-ray mapping. Unpublished MSc-ARST mini thesis, Mafokeng: University of the North West.

[Naz88] Nazaroff, W., Moed, B.A., Sextro, R.G. (1988) Soil as a source of indoor radon: Generation, migrations and entry. Radon and its decay products in indoor air. Editors W. Nazaroff and A. Nero, John Wiley and Sons, Inc., pp 60.

[Ner84] Nero, A.V., Nazaroff, W.W. (1984). Characterizing the source of radon indoors. Radiation Protection Dosimetry, Vol. 7, no. 1-4, pp 23 – 39.

[Ner88] Nero, A.V. (1988) Radon and its decay products in indoor air: An overview. Editors W. Nazaroff and A. Nero, John Wiley and Sons, Inc., pp 1 – 53.

[Nie96] Nielson, K.K., Rogers, V.C., Holl, R.B. (1996) Contributions of building materials to indoor radon levels in Florida buildings, USEPA Research and Development project summary, EPA/600/SR-96/107.

[Pal03] van der Pal, M. (2003) Radon transport in autoclaved aerated concrete. Published Doctorate thesis, Eindhoven: Technische Universiteit Eindhoven.

[Rad94] Rad Elec Inc. (1994), Reference Manual, Radon and Radiation Measurements.

[Sam84] Samuelsson, C., Petterson, H. (1984) Exhalation of ^{222}Rn from porous materials. Radiation Protection Dosimetry, Vol. 7, no.1 – 4, pp95 – 100.

[Sch94] Schumann, R.R., Gundersen, L.C.S., Tanner, A.B. (1994) Geology and occurrence of radon. In Radon: Prevalence, measurements, health risks and control. Editor N.L. Nageda, pp 83 – 96.

[Seg80] Segré, E. (1980) From X-rays to quarks: Modern physicists and their discoveries. W.H. Freeman and Company, San Francisco.

[Søg87] Søgaard-Hansen, J., Damkjær, A. (1987) Determining ^{222}Rn diffusion lengths in soils and sediments. Health Physics, Vol. 53, no. 5, pp 455 – 459.

[Spe03] Spelling, C. (2003) Mass, weight, density or specific gravity of water at various temperatures. (Online) http://www.simetric.co.uk/si_water.htm - ap, last updated 9 December 2003.

[Spo98a] van der Spoel, W.H., (1998) Radon transport in sand: A laboratory study. Doctorate thesis, Technische Universiteit Eindhoven.

[Spo98b] van der Spoel, W.H., van der Graaf, E.R., de Meijer, R.J. (1998). Combined diffusive and advective transport of radon in a homogenous column of dry sand. Health Physics, Vol. 74, no. 1, pp 48 – 63.

[Ste88] Steinhäusler, F. (1988) Epidemiological evidence of radon-induced health risks. Radon and its decay products in indoor air, Editors W. Nazaroff and A. Nero, John Wiley and Sons, Inc., pp 384.

[Ste92] Steinhäusler, F., Lettner, H. (1992) Radiometric survey in Namibia. Radiation Protection Dosimetry, Vol. 45, no. 1, pp 553 – 555.

[Str82] Strong, K.P., Levins, D.M. (1982) Effects of moisture content on radon emanation from uranium ore and tailings. Health Physics, Vol. 42, pp 27.

[Swa04] Swakoń, J., Kozak, K., Paszkowski, M., Gradziński, R., Łoskiewicz, J., Mazur, J., Janik, M., Bogacz, J., Horwacik, T., Olko, P. (2004). Radon concentration in soil gas around local disjunctive tectonic zones in the Krakow area. Journal of Environmental Radioactivity, Vol. 78, Issue 2, pp 137 – 149.

[Tan80] Tanner, A.B. (1980) Radon migration in the ground: A supplementary review. Proceedings of Natural Radiation Environment III: Springfield, US DOE Report CONF-780422, Vol. 1, pp 5 – 56.

[Vuz02] Vuza, H. M. (2002) Study of electret ion chambers as radon dosimeters in South Africa. M.Sc. thesis, University of the Western Cape, Bellville.

[Wik04] Wikipedia: The Free Encyclopedia (2004) (Online). http://en.wikipedia.org/wiki/Radon. Last updated 31 March.

[Wil00] William, R.F., Steck, D.J., Smith, B.J. (2000) Residential radon gas exposure and lung cancer. American Journal of Epidemiology, June issue.

Appendix A

The Calculation of the Radon Activity Concentration using Calibration Equations and Error Analysis

A.1 Radon Concentration Calculation

The E-PERM systems used in this study are designed to measure the radon concentration when exposed to air containing radon. The air enters into the chamber through diffusion on a molecular scale. The chambers are fitted with filtered inlets to capture the decay products that are present in the air that is being sampled. The electrostatic field caused by the electret collects the decay products from the radon decay. This causes a reduction in the surface charge of the electret. The decrease in voltage of the electret is then proportional to the radon concentration. A radon measurement involving the use of EIC (Electret Ion Chamber) radon monitors, involves 2 measurements of the surface voltage of the electret. The initial voltage (I) is taken before the exposure and the final voltage (F) reading is taken after exposure.

The E-PERM detectors are indifferent to extreme temperature changes [Kot00]. There is one minor change due to differences in thermal expansion coefficients, which might alter the shape of the electret and consequently give a varying surface voltage. The operation characteristics of the detector however, are unchanged [Liv90]. It is not the Teflon area that is affected, but the electret base material (the plastic holder that holds the electret). This identifies the importance that the surface voltages of the electrets should be measured at the same temperature. The initial and final voltages, together with experimentally determined calibration factors (CF) for each chamber

configuration are used to determine the radon activity concentration. The final equation to determine the radon concentration (RnC) is as follows

$$RnC = \frac{I - F}{CF \times T} - BG \qquad \text{(A.1)}$$

where RnC = radon concentration in Bq/m^3*

I = initial electret voltage in Volts

F = final electret voltage in Volts

CF = calibration factor for voltage drop in Volts/(Bq/m^3*days)

T = time in days

BG = environmental background correction in Bq/m^3.

A.2 Calibration Equations

The calibration factors for E-PERMs are defined as the decrease in electret voltage when a specific E-PERM configuration is exposed to a known radon concentration. Electrets discharge their surface voltages when exposed to ionising radiation, and as an example, the SST E-PERM loses 0.07 V per day for every 1 Bq/m^3 of radon [Kot88]. There is a nearly linear relationship between the calibration factor and the electret voltage in a range of about 150 – 750 Volts [Rad94]. It is for this reason that a self-correcting formula is used to get the actual calibration for a specific setup. The calibration equations vary for all combinations of chambers and electret types because of the varying voltage drops for each configuration. The following calibration equations are used to calculate the calibration factors. A blue labeled short-term electret fitted to a S chamber (SST) have the following calibration equation

$$CF = 1.69776 + 0.00057420 \times \frac{I + F}{2}. \qquad \text{(A.2)}$$

*The SI unit is Bq/m^3. To covert pCi/L to Bq/m^3, multiply by 37, i.e. 1 pCi/L = 37 Bq/m^3.

The SLT E-PERM configuration needs the following correction

$$CF = 0.14 + 0.0000525 \times \frac{I+F}{2}. \quad \text{(A.3)}$$

The LST E-PERM configuration needs the following adjustment

$$CF = 0.26127 + 0.0001386 \times \frac{I+F}{2} \quad \text{(A.4)}$$

where I and F is the initial and final voltages respectively. The above equations (A.2) to (A.4) are not listed in SI units, but in pCi/L units for easy reference to the E-PERM manual. The calibration factor (CF) is used in eq. (A.1) as is, but the final answer should be multiplied by 37 to get the result in Bq/m^3.

A.3 Background Corrections

Equation A.1 is used to determine the radon concentration and the environmental background should be subtracted from the apparent radon concentration. The only source of gamma radiation is from the natural background, unless the E-PERM detectors are exposed to a source emitting gamma radiation. A correction for this has to be made as in the case for different elevations [Kot92b]. The gamma background varies from place to place. The response for gamma radiation for the S chamber has a radon concentration equivalence of 3.2 Bq/m^3 for every 1 μR/h [Rad94]. The radon concentration equivalence of 1 μR/hour for the L chamber is 4.4 Bq/m^3. A typical range for gamma radiation varies from about 6 to 12μR/h. The effects of gamma radiation can also be measured using E-PERM detectors. The EICs are sealed in a Mylar bag, in a low radon environment and then exposed for periods up to a month. An average environmental level of about

10μR/h was used throughout this study in accordance with measurements in the laboratory at UWC [Vuz02].

A.4 Error Analysis for E-PERMs

In this section, the errors associated with E-PERMs are listed and their effect to the final radon concentration. The 3 sources of errors are identified as:

i. The error that is associated with faults in the system components (E_1). The imperfections include uncertainties in the volumes of the chambers, the thickness of the electrets and other possible problems like how tight the electret fit into the chamber. The contribution is about 5% [Kot92a].

ii. The second error component (E_2) includes the error in the electret voltage reading. The electret readers have an accuracy of ±1 Volt [Rad94], which is true for both the initial and final readings. The error for the 2 readings can be interpreted as the square root of the sum of the two 1 Volt errors. The final contribution is

$$E_2 = \frac{100 \times 1.4}{I - F}. \tag{A.5}$$

iii. The third component (E_3) stems from the uncertainty of the gamma background reading. In correcting for the environmental gamma background in Section A.3, a background correction factor was introduced. This is a result from a compilation of average background data. The error involving the variations were of minimal contributions, about 4 – 7 Bq/m^3 [Rad94]. The error can of course be minimised if the exact gamma contribution is known, but for using the average contribution, the error is about

$$E_2 = \frac{100 \times 7}{RnC} \tag{A.6}$$

where the 7 Bq/m^3 arises from the background correction and RnC is the radon concentration.

The total error from the above mentioned components add up to the following

$$E_{Total}(\%) = \sqrt{(E_1)^2 + (E_2)^2 + (E_3)^2} \tag{A.7}$$

or

$$E_{Total}(\%) = \sqrt{(5)^2 + (\frac{100 \times 1.4}{I - F})^2 + (\frac{100 \times 7}{RnC})^2} \ . \tag{A.8}$$

Appendix B

B.1 Map of Kloof Gold Mine Dump No.1

A construction map of the inactive gold tailings dam at Kloof Gold Mine. Kloof falls under the Gold Fields Limited group and the Kloof Division process a life-of-mine grade of 13.9 g/t gold [Cha03]. The black arrow on the figure indicates north.

Appendix C

C.1 Radon concentrations C(z) calculated from eq. (3.19) with different values of *l*.

Z-Values	C (z) - 0.5m	C (z) - 1.0m	C (z) - 1.5m	C (z) - 2.0m	C (z) - 2.5m	C (z) - 3.0m
0	10	10	10	10	10	10
0.10	89955	47229	32011	24210	19466	16277
0.20	163597	89955	61949	47229	38160	32011
0.30	223889	128616	89955	69126	56120	47229
0.40	273252	163597	116156	89955	73376	61949
0.50	313667	195249	140667	109769	89955	76185
0.60	346756	223889	163597	128616	105885	89955
0.70	373847	249803	185048	146543	121190	103274
0.80	396027	273252	205115	163597	135894	116156
0.90	414187	294469	223889	179818	150022	128616
1.00	429055	313667	241452	195249	163597	140667
1.10	441228	331038	257882	209927	176638	152323
1.20	451194	346756	273252	223889	189169	163597
1.30	459354	360978	287631	237170	201208	174501
1.40	466034	373847	301083	249803	212775	185048
1.50	471504	385491	313667	261821	223889	195249
1.60	475982	396027	325440	273252	234567	205115
1.70	479648	405561	336453	284126	244826	214659
1.80	482650	414187	346756	294469	254683	223889
1.90	485108	421992	356395	304308	264153	232817
2.00	487120	429055	365412	313667	273252	241452
2.10	488767	435445	373847	322570	281994	249803
2.20	490116	441228	381739	331038	290394	257882
2.30	491220	446460	389121	339094	298464	265695
2.40	492125	451194	396027	346756	306217	273252
2.50	492865	455478	402488	354045	313667	280561
2.60	493471	459354	408533	360978	320825	287631
2.70	493967	462861	414187	367574	327701	294469
2.80	494373	466034	419477	373847	334309	301083
2.90	494706	468906	424426	379815	340657	307480
3.00	494978	471504	429055	385491	346756	313667
3.10	495201	473855	433386	390891	352616	319651
3.20	495384	475982	437438	396027	358247	325440
3.30	495533	477907	441228	400913	363656	331038
3.40	495655	479648	444774	405561	368854	336453
3.50	495756	481224	448091	409982	373847	341690
3.60	495838	482650	451194	414187	378645	346756
3.70	495905	483940	454097	418187	383255	351656
3.80	495960	485108	456813	421992	387684	356395
3.90	496005	486164	459354	425612	391939	360978
4.00	496042	487120	461731	429055	396027	365412
4.10	496072	487985	463954	432330	399956	369700
4.20	496097	488767	466034	435445	403730	373847
4.30	496117	489475	467980	438409	407356	377859
4.40	496133	490116	469801	441228	410840	381739
4.50	496147	490696	471504	443909	414187	385491
4.60	496158	491220	473097	446460	417403	389121
4.70	496167	491695	474588	448886	420493	392632
4.80	496175	492125	475982	451194	423462	396027
4.90	496181	492513	477286	453389	426314	399312
5.00	496186	492865	478507	455478	429055	402488

Table C.1 The assumed constant parameters of the mine dump soil used in the modelling calculations in predicting the maximum radon concentration.

Radon emanation coefficient	η	0.3
Specific bulk density	ρ_s	2846 kg/m^3
Radium content	A_{Ra}	310 Bq/kg
Soil porosity	ε	0.35

The radium content was taken from [Mot03] as the average content was measured from at least 17 soil samples collected all over the dump. The specific bulk density was of that calculated in this study, as well as the porosity. Equation (3.16) will be used to do the final calculation.

$$C_{\max} = \frac{S}{\lambda}. \tag{3.16}$$

where S is defined by equation (3.16),

$$S = \frac{\eta \rho_s \lambda_{Rn} A_{Ra} (1-\varepsilon)}{\varepsilon}. \tag{3.17}$$

Substituting the parameters above into both these equations, yields a concentration (C_{max}) of about 491 544 Bq/m^3.